SUPPLEMENTARY INFORMATION

Azetidinyl Malachite Green: a Superior Fluorogen-Activating Protein Probe for Live-cell and Dynamic SIM Imaging

Fei Deng,‡ [abc] Xiangning Fang,‡[ae] Qinglong Qiao,*[a] Guoli Han,[ae] Lu Miao,[a] Shuangshuang Long [ad] and Zhaochao Xu*[ae]

[a]CAS Key Laboratory of Separation Science for Analytical Chemistry, Dalian Institute of Chemical Physics, Chinese Academy of Sciences, Dalian 116023, China.
[b]School of Chemistry and Chemical Engineering, Jinggangshan University, Ji'an, Jiangxi 343009, China.
[c]Key Laboratory of Jiangxi Province for Special Optoelectronic Artificial Crystal Materials, Ji'an, Jiangxi 343009, China.
[d]School of Chemistry and Chemical Engineering, University of South China, Hengyang, Hunan 421001, China.
[e]University of Chinese Academy of Sciences, Beijing 100049, China.

‡ These two authors contributed equally.
*Corresponding authors
E-mail addresses: qqlqiao@dicp.ac.cn (Q. Qiao), zcxu@dicp.ac.cn (Z. Xu)

Table of Contents

1 Materials and instruments

Unless otherwise stated, all reagents and solvents for synthesis and detection were purchased from commercial suppliers (J&K, Adamas, Innochem, and Aladdin) and used without further purification. All water used was from Millipore water purification system with a minimum resistivity of 18.0 MΩ·cm. The plasmids pET21-10XHis-GST-HRV-dL5 (bacterial expression vector for dL5**), pcDNA3.1-NLS-myc-dL5-2xG4S-mCer3 (expresses myc-dL5**-mCer3 fusion protein in nuclei), pcDNA3.1-COXIV-COX8-dL5-2XG4S-mCer3 (expresses dL5**-mCer3 fusion protein in mitochondria) and pcDNA3.1-kappa-myc-dL5-2XG4S-mCer3-KDEL (expresses myc-dL5**-mCer3 fusion protein in endoplasmic reticulum) were obtained from Addgene.

^{1}H NMR and ^{13}C NMR spectra were recorded on Bruker 400 spectrometer. Mass spectrometry data were obtained with Agilent 6540 LC/QTOF and AB SCIEX MALDI-TOF/TOF 5800. UV-Vis absorption spectra were collected on Agilent Cary 60 UV-Vis Spectrophotometer. Fluorescence measurements were performed on Agilent CARY Eclipse and HORIBA FluoroMax-4 fluorescence spectrophotometers. Confocal images were performed on Laser Scanning Confocal Microscope (Andor iQ 3.2) with 100×oil-immersion objective lens. Structured illumination microscopy (SIM) super-resolution images were taken on a Nikon N-SIM system with a 100×oil immersion objective lens, 1.49 NA (Nikon). Images were captured using Nikon NISElements and reconstructed using slice reconstruction in NIS-elements.

2 Synthesis of MGs

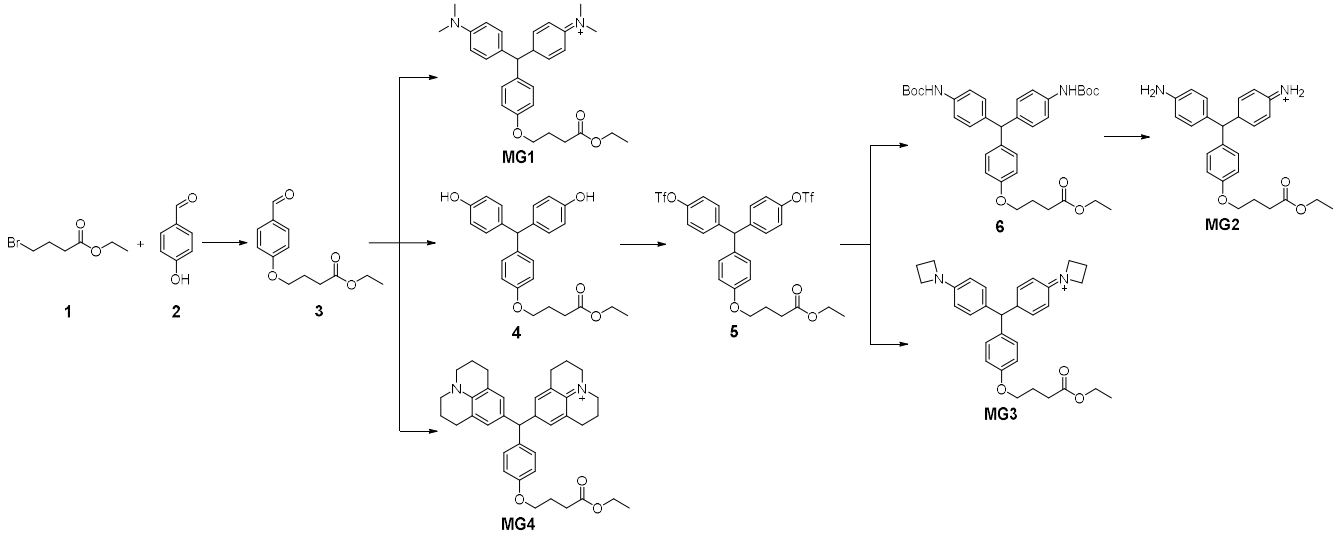

Scheme S1. Synthesis of **MG1-4**

Compound 3. This compound was synthesized according to a previously reported procedure.[1] ^{1}H NMR (400 MHz, $CDCl_3$) δ 9.88 (s, 1H), 7.83 (d, *J* = 8.7 Hz, 2H), 6.99 (d, *J* = 8.7 Hz, 2H), 4.31 – 3.99 (m, 4H), 2.53 (t, *J* = 7.2 Hz, 2H), 2.25 – 2.09 (m, 2H), 1.26 (t, *J* = 7.1 Hz, 3H).

MG1. This compound was synthesized according to a previously reported procedure.[2] ^{1}H NMR (400 MHz, CD_3CN) δ 7.33 (dd, *J* = 22.2, 8.6 Hz, 6H), 7.11 (d, *J* = 8.0 Hz, 2H), 6.95 (d, *J* = 8.9 Hz, 4H), 4.28 – 3.97 (m, 4H), 3.26 (s, 12H), 2.50 (t, *J* = 7.2 Hz, 2H), 2.10 (t, *J* = 6.7 Hz, 2H), 1.23 (t, *J* = 7.1 Hz, 3H).

Compound 4. Compound **3** (1.1 g; 5 mmol), phenol (1.88 g, 20 mmol) and *p*-toluenesulfonic acid monohydrate (95 mg, 0.5 mmol) were dissolved in 20 mL toluene. The reaction mixture were stirred at 60 ℃ for 20 h. After cooling to room temperature, the reaction mixture was concentrated under reduced pressure. The residue was purified by column chromatography on silica gel to afford the desired compound (1.32 g, 65%). ^{1}H NMR (400 MHz, $CDCl_3$) δ 6.90 (dd, *J* = 23.4, 8.2 Hz, 6H), 6.71 (dd, *J* = 15.1, 8.2 Hz, 6H), 6.35 (s, 2H), 5.24 (s, 1H), 4.12 (q, *J* = 7.1 Hz, 2H), 3.91 (t, *J* = 6.0 Hz, 2H), 2.49 (t, *J* = 7.3 Hz, 2H), 2.05 (p, *J* = 6.7 Hz, 2H), 1.21 (t, *J* = 7.1 Hz, 3H). ^{13}C NMR (100 MHz, $CDCl_3$) δ 174.50, 157.02, 153.96, 137.06, 136.72, 130.41, 130.27, 115.21, 114.28, 66.78, 61.05, 54.36, 31.09, 24.68, 14.18. HRMS (ESI) calcd. for $C_{25}H_{27}O_5^+$ $[M+H]^+$ 407.1858, found 407.1866.

Compound 5. Compound **4** (0.61 g; 1.5 mmol) was dissolved in 20 mL dichloromethane and cooled to 0 °C. After the addition of pyridine (0.95 g; 12 mmol) and Tf_2O (1.7 g; 6 mmol), the reaction was slowly warmed to room temperature and stirred for another 1 h. The reaction was quenched with water (30 mL) and extracted with dichloromethane (3 × 30 mL). The organic layers were combined and dried over Na_2SO_4. After filtration and removal of the solvent under reduced pressure, the residue was purified by column chromatography on silica gel to afford the desired compound (0.95 g, 95%). ^{1}H NMR (400 MHz, MeOD) δ 7.37 – 7.21 (m, 8H), 7.00 (d, *J* = 8.7 Hz, 2H), 6.87 (d, *J* = 8.7 Hz, 2H), 5.67 (s, 1H), 4.11 (q, *J* = 7.2 Hz, 2H), 3.98 (t, *J* = 6.2 Hz, 2H), 2.48 (t, *J* = 7.3 Hz, 2H), 2.14 – 1.92 (m, 2H), 1.22 (t, *J* = 7.1 Hz, 3H). ^{13}C NMR (101 MHz, MeOD) δ 173.62,

157.89, 148.22, 144.58, 134.47, 130.92, 129.92, 121.04, 120.34, 117.17, 114.33, 66.58, 60.14, 54.30, 30.30, 24.41, 13.10. HRMS (ESI) calcd. for $C_{27}H_{25}F_6O_9S_2^+$ $[M+H]^+$ 671.0844, found 671.0895.

Compound 6. Compound **5** (134 mg, 0.2 mmol), $Pd_2(dba)_3$ (37 mg, 0.04 mmol), Cs_2CO_3 (162 mg, 0.5 mmol), tBuXPhos (25 mg, 0.06 mmol) and tert-Butyl carbamate (56 mg, 0.48 mmol) were added to a 25 mL flask. The flask was sealed and evacuated/backfilled with nitrogen (3 x). Dioxane (2 mL) was added and the mixture was stirred at 100 ℃ for 18 h. After cooling to room temperature, the reaction mixture was concentrated under reduced pressure. The residue was purified by column chromatography on silica gel to afford the desired compound (70 mg, 58%). ^{1}H NMR (400 MHz, $CDCl_3$) δ 7.24 (s, 2H), 6.98 (dd, *J* = 11.5, 8.6 Hz, 6H), 6.78 (d, *J* = 8.7 Hz, 2H), 6.43 (s, 2H), 5.38 (s, 1H), 4.14 (q, *J* = 7.1 Hz, 2H), 3.97 (t, *J* = 6.1 Hz, 2H), 2.50 (t, *J* = 7.3 Hz, 2H), 2.09 (p, *J* = 6.7 Hz, 2H), 1.50 (s, 18H), 1.25 (t, *J* = 7.1 Hz, 3H). ^{13}C NMR (100 MHz, $CDCl_3$) δ 173.26, 157.24, 152.81, 139.05, 136.45, 136.32, 130.25, 129.81, 118.52, 114.18, 80.44, 66.67, 60.42, 54.70, 30.86, 28.35, 24.70, 14.24.

MG2. Compound 6 (70 mg, 0.12 mmol) was dissolved in 2.5 mL dichloromethane and 0.5 mL trifluoroacetic acid was added. The reaction mixture was stirred at room temperature for 12 h. After concentrating under reduced pressure, DDQ and methanol (5 mL) were added and stirred at room temperature for 1 hour. After removal of the solvent under reduced pressure, the residue was purified by column chromatography on silica gel to afford the desired compound (42 mg, 70%). ^{1}H NMR (400 MHz, MeOD) δ 7.34 (dd, *J* = 15.3, 8.8 Hz, 6H), 7.16 (d, *J* = 8.8 Hz, 2H), 6.85 (d, *J* = 8.9 Hz, 4H), 4.26 – 4.03 (m, 4H), 2.55 (t, *J* = 7.2 Hz, 2H), 2.15 (t, *J* = 6.7 Hz, 2H), 1.26 (t, *J* = 7.1 Hz, 3H). ^{13}C NMR (100 MHz, MeOD) δ 179.37, 173.43, 164.27, 159.42, 141.41, 137.49, 131.75, 127.00, 114.83, 114.53, 67.36, 60.23, 30.13, 24.19, 13.12. HRMS (ESI) calcd. for $C_{25}H_{27}N_2O_3^+$ $[M]^+$ 403.2016, found 403.2015.

MG 3. Compound **5** (134 mg, 0.2 mmol), $Pd_2(dba)_3$ (37 mg, 0.04 mmol), Cs_2CO_3 (162 mg, 0.5 mmol) and tBuXPhos (25 mg, 0.06 mmol) were added to a 25 mL flask. The flask was sealed and evacuated/backfilled with nitrogen (3 x). Dioxane (2 mL) and azetidine (27 mg, 0.48 mmol) were added and the mixture was stirred at 100 ℃ for 18 h. The mixture was subsequently cooled to room temperature and diluted with 10 mL MeOH, then DDQ (90 mg, 0.4 mmol) was added and stirred for 2 h. After filtration and removal of the solvent under reduced pressure, the residue was purified by column chromatography on silica gel to afford the desired compound (45 mg, 43%).^{1}H NMR (400 MHz, MeOD) δ 7.32 (dd, *J* = 11.6, 8.9 Hz, 6H), 7.13 (d, *J* = 8.8 Hz, 2H), 6.72 – 6.43 (m, 4H), 4.31 (t, *J* = 7.6 Hz, 8H), 4.23 – 4.10 (m, 4H), 2.55 (q, *J* = 7.7, 7.3 Hz, 6H), 2.19 – 2.09 (m, 2H), 1.25 (t, *J* = 7.2 Hz, 3H). ^{13}C NMR (101 MHz, MeOD) δ 177.63, 173.42, 163.94, 156.04, 140.21, 137.17, 131.92, 126.91, 114.52, 111.01, 67.34, 60.23, 51.44, 30.14, 24.21, 15.55, 13.15. HRMS (ESI) calcd. for $C_{31}H_{35}N_2O_3^+$ $[M]^+$ 483.2642, found 483.2688.

MG 4. Compound 3 (236 mg, 1 mmol), julolidine (347 g, 2 mmol) and p-toluenesulfonic acid monohydrate (190 mg, 1 mmol) were dissolved in 10 mL toluene. The reaction mixture were stirred at 100 ℃ for 12 h. After cooling to room temperature, the reaction mixture was concentrated under reduced pressure. The residue was diluted with 10 mL MeOH, then DDQ (246 mg, 1 mmol) was added and reflux for 2 h. After removal of the solvent under reduced pressure, the residue was purified by column chromatography on silica gel to afford the desired compound (190 mg, 32%). ^{1}H NMR (400 MHz, MeOD) δ 7.22 (d, *J* = 8.0 Hz, 2H), 7.10 (d, *J* = 8.8 Hz, 2H), 6.91 (s, 4H), 4.29 – 4.13 (m, 4H), 3.55 (t, *J* = 5.8 Hz, 8H), 2.75 (t, *J* = 6.2 Hz, 8H), 2.57 (t, *J* = 7.2 Hz, 2H), 2.23 – 2.11 (m, 2H), 2.09 – 1.93 (m, 8H), 1.28 (t, *J* = 7.2 Hz, 3H). ^{13}C NMR (101 MHz, MeOD) δ 175.14, 174.89, 164.52, 152.53, 138.20, 137.96, 133.69, 129.75, 127.90, 126.95, 124.12, 115.62, 68.62, 61.65, 52.00, 31.60, 28.40, 25.66, 21.89, 14.55. HRMS (ESI) calcd. for $C_{37}H_{43}N_2O_3^+$ $[M]^+$ 563.3268, found 563.3271.

3 Experimental Procedures

3.1 Expression and purification of dL5**

Competent Cells BL21 (Takara) were transformed with pET21-10XHis-GST-HRV-dL5 and selected for ampicillin resistance yielding E. coli_dL5**. The fresh colonies were grown in 5 mL LB containing 50 μg/mL ampicillin overnight. The 5 mL overnight cultures were then added to 500 mL LB (containing 50 μg/mL ampicillin) and culture to an OD of 0.8 at 37°C. The expression of dL5** was induced by the addition of 500 μM IPTG and kept at 20°C for 12 h. The cells were centrifuged and resuspended in 20 mL buffer A (20 mM Tris, 500 mM NaCl, 5 mM imidazole pH7.5). The cells were disrupted by sonication at 4°C. This lysate was centrifuged 30 min at 20 000g and the supernatant was incubated with buffer A prewashed Ni-NTA-agarose for 2h at 4°C. After binding, the Ni-NTA-agarose were washed with buffer 60 (same as wash buffer A but with 60 mM imidazole) and eluted with buffer 200 (same as wash buffer A but with 200 mM imidazole) to get His-GST tagged dL5**. The His-GST were cleaved from dL5** through His tagged HRV 3C protease (Takara) at 4°C overnight. Finally, dL5** was purified by column chromatography on Ni-NTA-agarose. Protein concentration was determined using a BCA protein assay kit (Sangon Biotech).

3.2 Spectral measurements

MGs were dissolved in DMSO to afford 2 mM stock solutions. The **MGs** were diluted to 0.5 μM with PBS buffer solution (pH 7.40) for intrinsic absorbance and fluorescence measurements. The absorbance and fluorescence measurements of **MGs**/dL5** were carried out using 2 μM dL5** and 0.5 μM **MGs**.

3.3 Determination of Φ and K_d

The fluorescence quantum yields (Φ) were determined using Si-rhodamine (Φ = 0.41 in PBS pH 7.40) [3] as the standard and calculated using the following equation:

$$\Phi_s = \Phi_r \times \frac{A_r F_s n_s^2}{A_s F_r n_r^2}$$

where, the subscripts "s" and "r" stand for sample and reference, respectively. A is the absorbance. F is the integrated fluorescence intensity and n is the refractive index of the solvent.

Binding affinity to dL5** was determined by measuring fluorescence intensity at λ_{max} under conditions of ligand depletion. 10 nM dL5** were each assayed with a 0 to 500 nM range of **MGs**. K_d values were determined by non-linear regression using the following equation [2]:

$$F = \frac{c + K_d + R - \sqrt{(c + K_d + R)^2 - 4cR}}{2}$$

where R stand for fluorescence intensity of **MGs**/dL5** complex at the observed or extrapolated plateau.

3.4 Quantum chemical calculations

All the quantum chemical calculations were carried out at the ORCA 5.0.0 [4-6] program package using density functional theory (DFT) or time-dependent density functional theory (TD-DFT). The ground states geometries of **MGs** were optimized at r^{2}SCAN-3c [7] composite method. Single point energies of the optimized structures were further calculated at RI-ωB97M-V/def2-TZVP level. The excited states were calculated at RI-PBE0/def2-SV(P) level. All the calculations were conducted in conductor-like polarizable continuum model (CPCM) of water. The corresponding molecular orbital composition, absorption were analyzed by Multiwfn [8]. Molecular representations were conducted by VMD [9].

3.5 Molecular docking

The protein structure homology-modelling of dL5** were constructed through SWISS-MODEL [10] using **MG1**-bound L5* (PDB ID: 4K3H) as the template. Automated docking simulations were conducted with AutoDock Vina [11]. The best conformation of the docking complex was generated based on the scoring functions and visualized via PyMOL [12].

3.6 Cell cultures and imaging experiments

About 2 × 10^4 Hela cells were seeded into confocal dish (35 mm, NEST) and cultured in Dulbecco's modified Eagle's medium (DMEM, Gibco) supplied with 10% fetal bovine serum (FBS, Gibco) under standard culture conditions (atmosphere of 5% CO_2 and 95% air at 37°C) for 48 h. The plasmids pcDNA3.1-NLS-myc-dL5-2xG4S-mCer3, pcDNA3.1-COXIV-COX8-dL5-2XG4S-mCer3 and pcDNA3.1-kappa-myc-dL5-2XG4S-mCer3-KDEL were transfected Hela cells by using Lipofectamine 2000 (Invitrogen) according to the manufacturer's protocol. After the incubation of the cells at 5 % CO_2 37 °C for 24 h, the cells were then rinsed twice with PBS and incubated with FBS-free DMEM containing **MGs** (200 nM) for 15 min. After incubation, cells were rinsed with PBS twice again for live-cell imaging. For photostability assessment, Hela cells were incubated with 4% paraformaldehyde for 10 min and 0.1% TritonX-100 for 2 min respectively. The fixed Hela cells were rinsed twice with PBS and incubated with PBS containing MGs (200 nM) for 15 min. In the experimental group, the cells were imaged directly under continuous 640 nm laser irradiation. In contrast, cells in the control group were imaged after washing excess MGs with PBS.

4 Results and Discussion

4.1 Characterization of dL5**

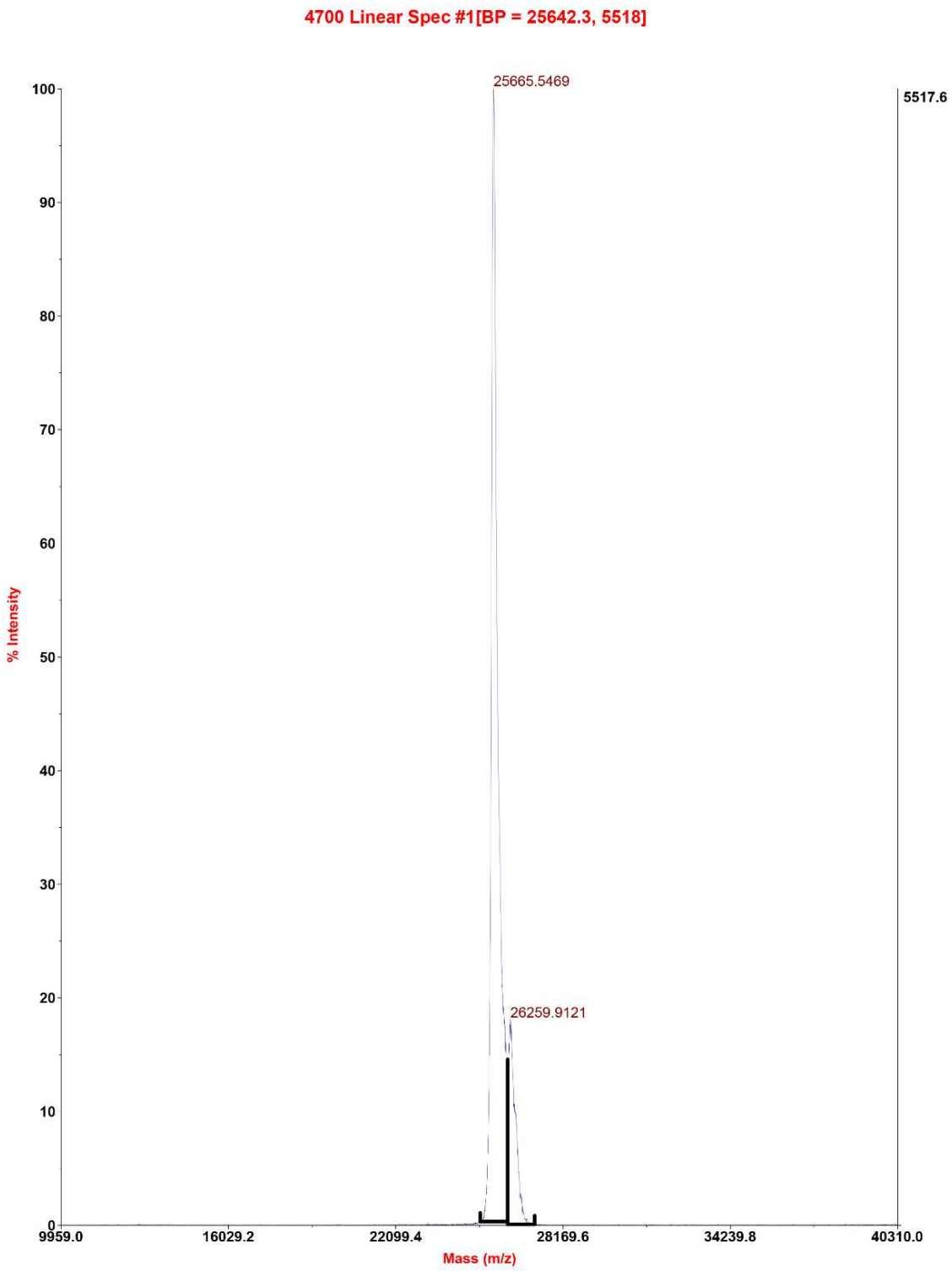

Figure S1. MALDI-TOF-MS data of dL5**

4.2 Spectroscopic characterizations of MGs and MGs/dL5**

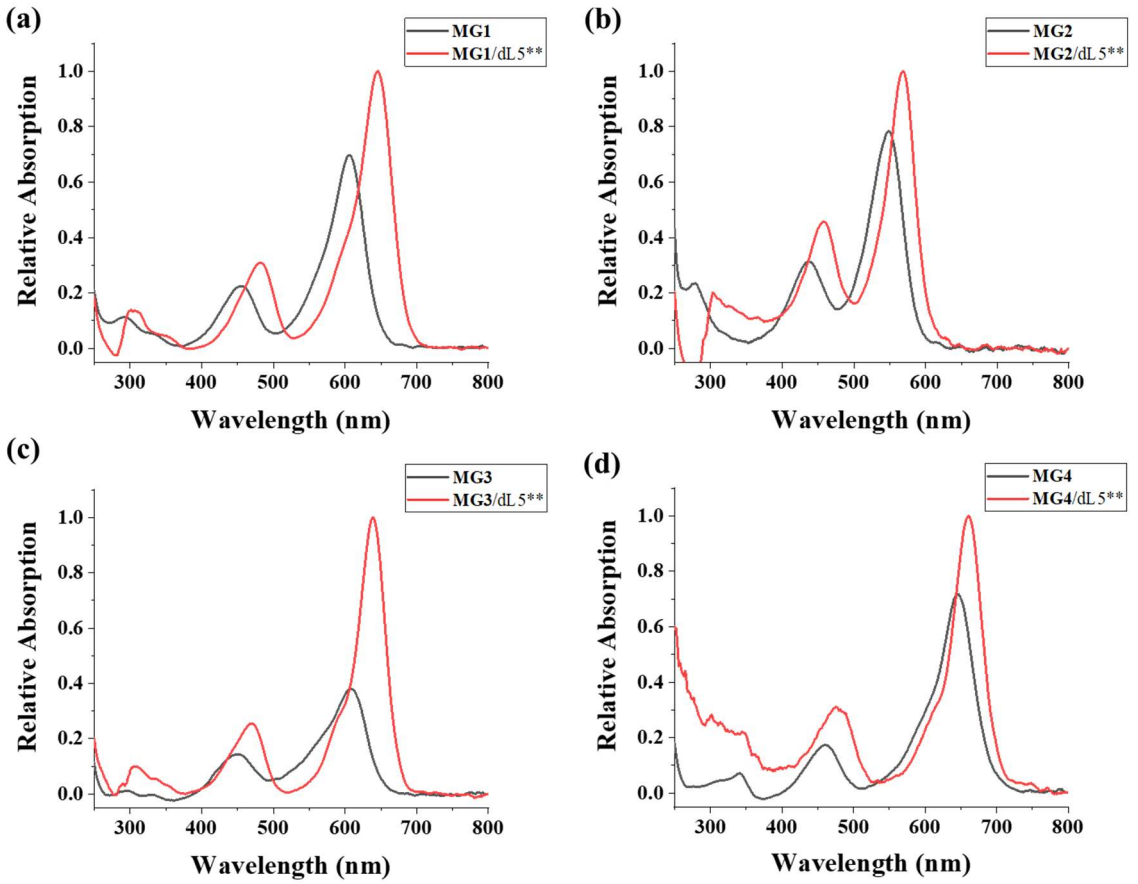

Figure S2. Absorption spectra of **MGs** and **MGs**/dL5**.

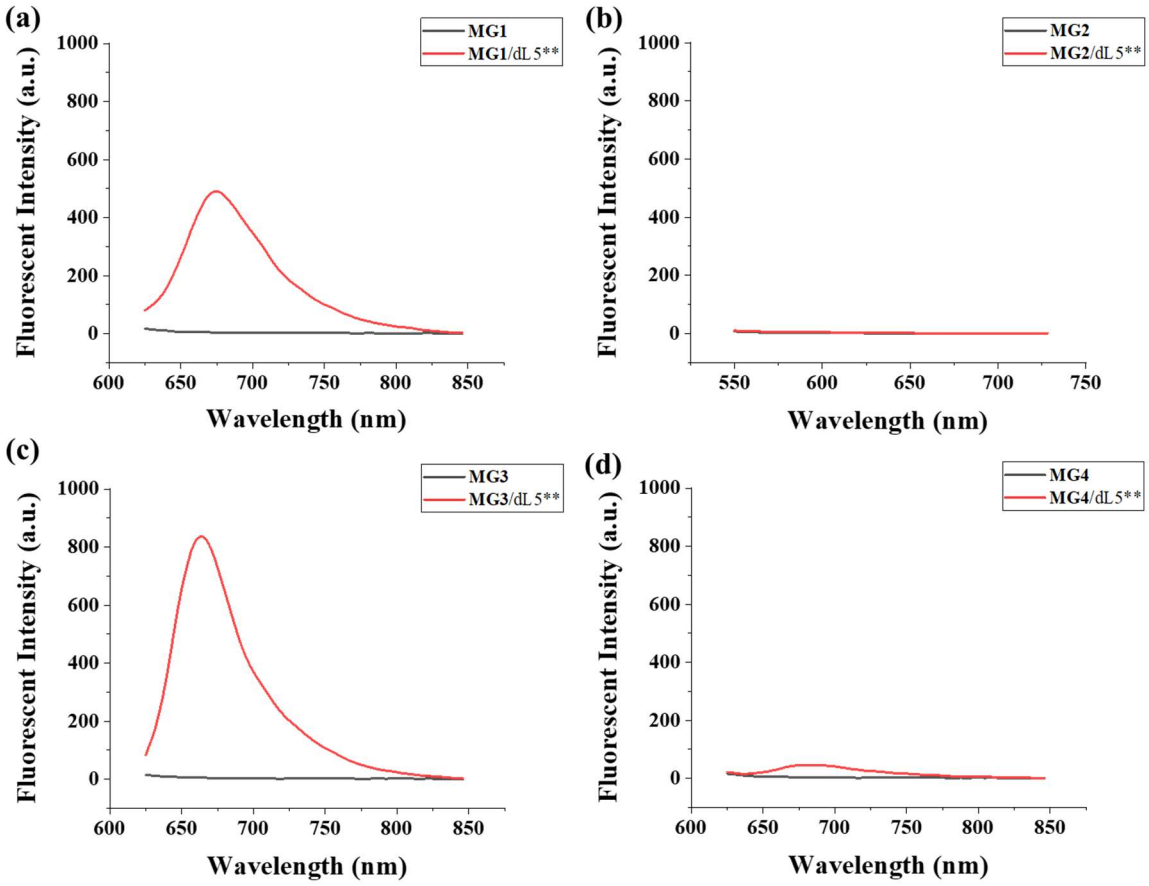

Figure S3. fluorescence spectra of **MGs** and **MGs**/dL5**.

Table S1 Correlation between shifts in the absorption maximum and the calculated binding energy.

Dye	$\Delta\lambda_{abs}$ (nm)	Affinities (kcal/mol)
MG1	40	-10.8
MG2	20	-9.8
MG3	32	-10.4
MG4	15	-2.5

4.3 Binding affinity of MGs to dL5**

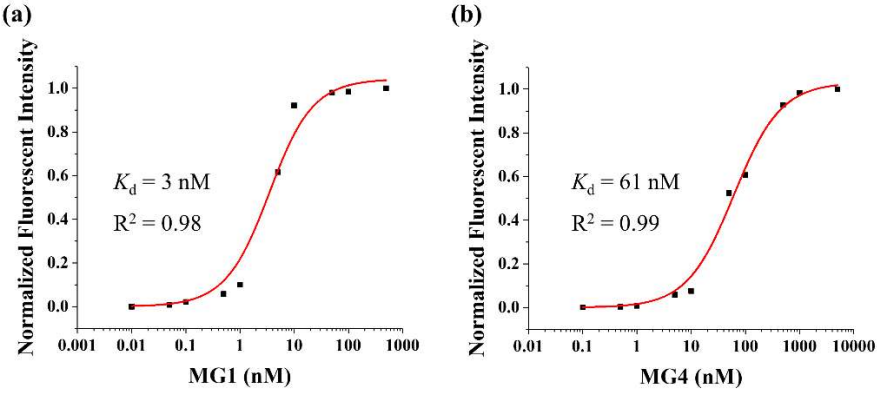

Figure S4. Binding equilibrium analysis of **MG1** and **MG4** to dL5**.

4.4 Photostability of MG1/dL5 and MG3/dL5** in confocal microscopy**

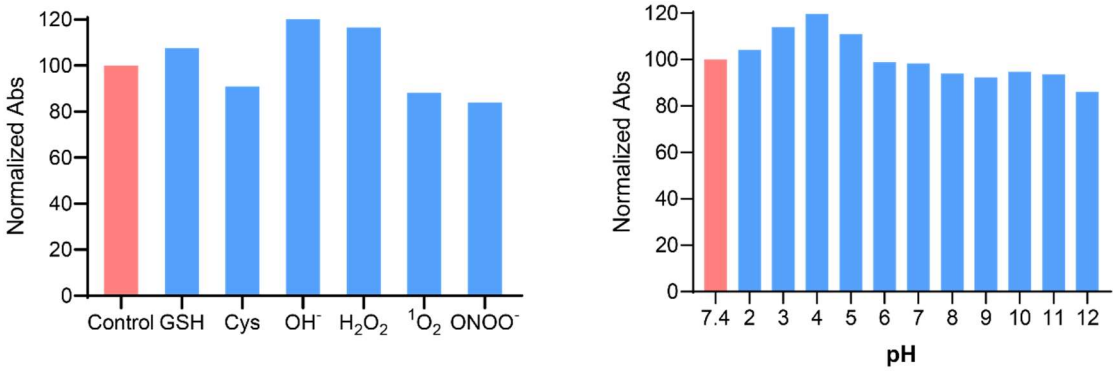

Figure S5. The stability of MG3 in the presence of different biological interferences and in various pH values. The stability of **MG3** was evaluated in the presence of reactive oxygen species (ROS) (10 μM $^1O_2$, 100 mM OH^-), reactive nitrogen species (RNS) (10 μM $ONOO^-$), and reactive sulfur species (RSS) (100 mM GSH, 200 μM Cys). The selected concentrations of these biological interferences are significantly higher than typical physiological levels, providing further insights into the molecule's stability in live cells. We assessed the absorbance of **MG3** at 607 nm to evaluate its stability in the presence of these different biological interferences. The results indicated that **MG3** exhibited negligible absorbance changed in the presence of different biological interferences (Figure S5a). We also tested the absorbance of **MG3** across different pH levels using citrate buffer and phosphate buffer to further evaluate its stability. The absorbance intensity at 607 nm of **MG3** at physiological pH (7.4) was used as a control. The normalized absorbance of **MG3** at various pH levels is presented in Figure S5b, showing only slight variation within the pH range of 2 to 12. These results demonstrate that MG3 remains stable across a wide range of pH values.

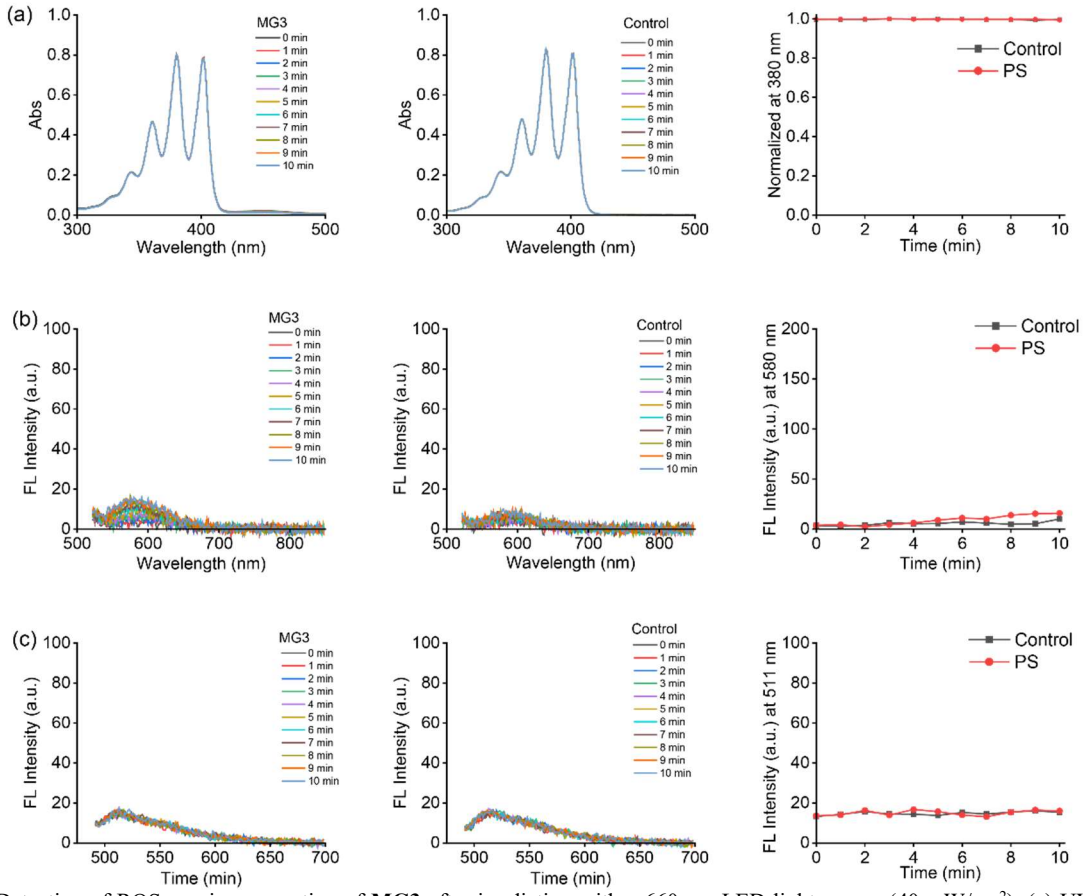

Figure S6. Detection of ROS species generation of **MG3** after irradiation with a 660 nm LED light source (40 mW/cm^2). (a) UV-vis absorption spectra of PBS solution containing 70 μM ABDA after irradiation at 660 nm for different time periods. (b) Fluorescence emission spectra of PBS solution containing 40 μM DHE after irradiation at 660 nm for different time periods. (c) Fluorescence emission spectra of PBS solution containing 40 μM HPF after irradiation at 660 nm for different time periods.

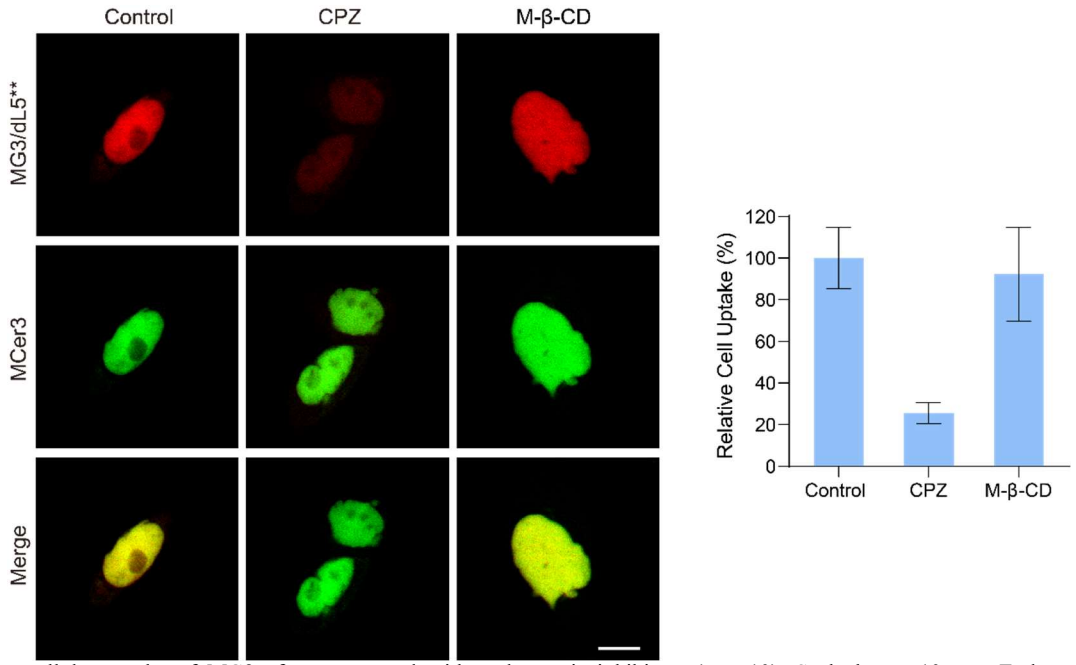

Figure S7. The cellular uptake of MG3 after pre-treated with endocytosis inhibitors (n = 10). Scale bar = 10 μm. Endocytosis inhibitors chlorpromazine (CPZ) and methyl-β-cyclodextrin (M-β-CD) were utilized to investigate the cellular uptake mechanism of **MG3**. CPZ is known as a clathrin-mediated endocytosis inhibitor, while M-β-CD acts as a lipid raft inhibitor. HeLa cells were incubated with CPZ (15 μg/mL) and M-β-CD (100 μg/mL) for 1 hour. Following this treatment, the culture medium was replaced with fresh medium containing **MG3** (200 nM) for an additional 30 minutes. Confocal imaging was then performed to elucidate the endocytosis pathways associated with **MG3** uptake. To account for potential variability in the expression levels of dL5** protein among individual cells, we evaluated the cellular uptake of **MG3** by calculating the fluorescence

intensity ratio of MG3 (640 nm channel) to mCer3 (405 nm channel). The results showed that the fluorescence intensity ratio in cells treated with CPZ decreased to 25% compared to the control group, while cells treated with M-β-CD maintained a nearly constant ratio. These findings suggest that the cellular uptake of **MG3** is primarily mediated by clathrin-dependent endocytosis.

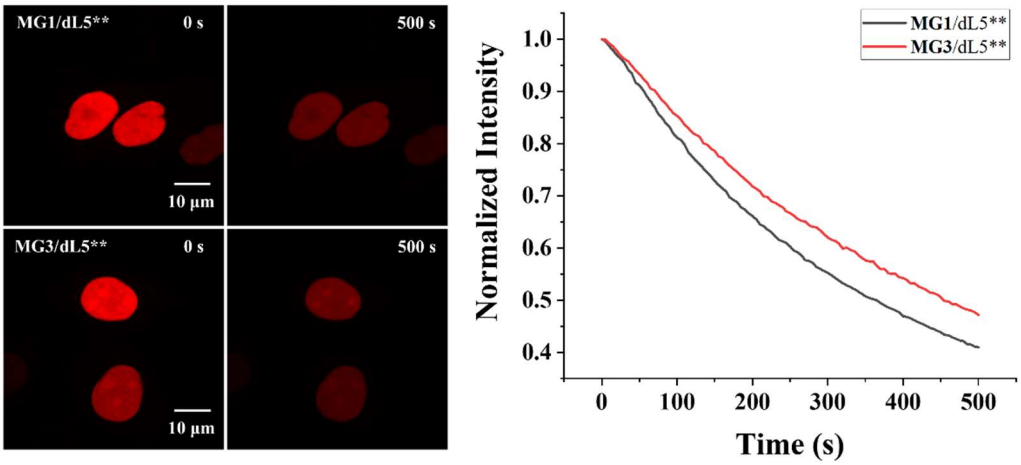

Figure S8. Quantification of the relative fluorescent intensity of MG1/dL5** and MG3/dL5** in Hela cells with continuous irradiation using confocal microscopy.

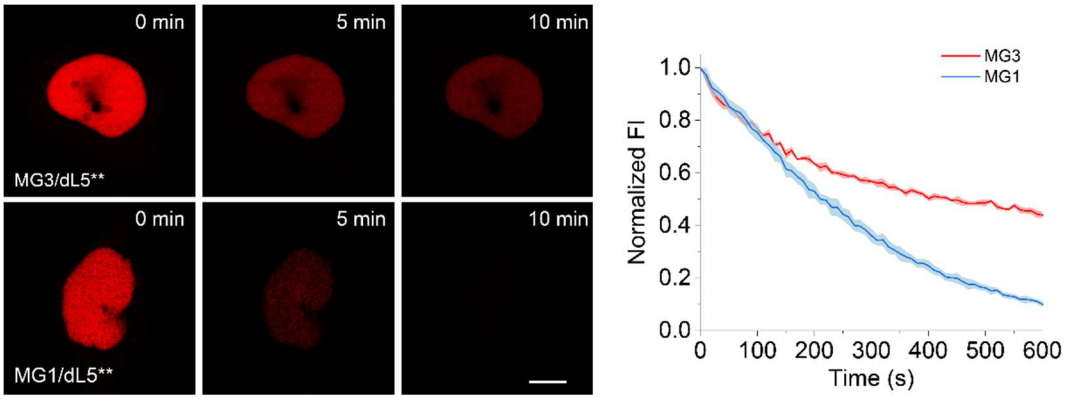

Figure S9. Quantification of the relative fluorescent intensity of **MG1**/dL5** and **MG3**/dL5** in Hela cells with continuous irradiation by confocal imaging. Scale bar = 10 μm.

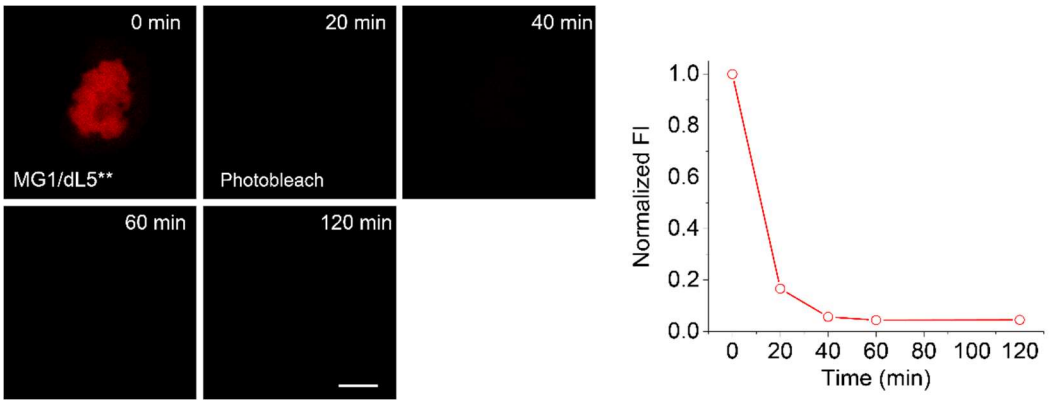

Figure S10. Fluorescence variation of **MG1**/dL5** in Hela cells after 20 min continuous irradiation of 640 nm laser. Scale bar = 10 μm.

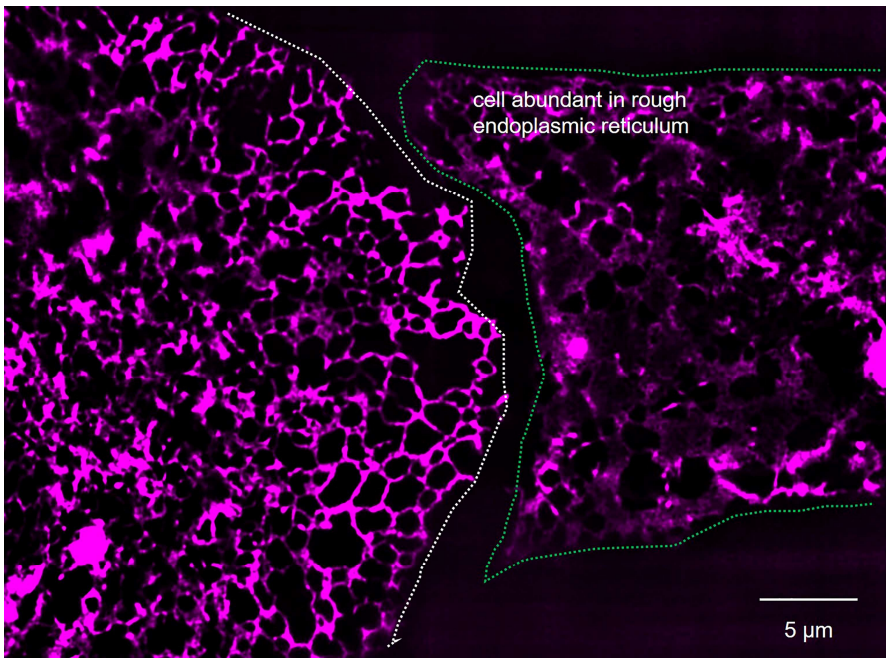

Figure S11. SIM imaging of endoplasmic reticulum in living HeLa cells with **MG3**.

4.5 Results of quantum chemical calculations

4.5.1 Geometry optimization

Table S2. Calculated atomic coordinates of **MG1**.

Atom#	Symbol	X	Y	Z
1	C	1.390701	4.703638	-2.01713
2	C	1.81887	3.349515	-2.13347
3	C	0.987547	2.317446	-1.78238
4	C	-0.33694	2.539643	-1.32159
5	C	-0.75479	3.892013	-1.21099
6	C	0.072322	4.937707	-1.52943
7	C	-1.20039	1.453713	-0.97543
8	C	-2.62041	1.565471	-1.1092
9	C	-3.21701	2.38671	-2.10128
10	C	-4.57728	2.490522	-2.23816
11	C	-5.45473	1.791853	-1.35952
12	C	-4.86494	0.966175	-0.35926
13	C	-3.50258	0.850013	-0.25788
14	N	-6.79503	1.90303	-1.47487
15	N	2.205124	5.726618	-2.35074
16	C	1.730033	7.1085	-2.28722
17	C	3.582882	5.476062	-2.77337
18	C	-7.68462	1.122015	-0.61595
19	C	-7.38467	2.80871	-2.46014
20	C	-0.62553	0.21196	-0.47987
21	C	-1.16892	-1.03897	-0.84524
22	C	-0.61476	-2.21617	-0.39243
23	C	0.494539	-2.18605	0.468997
24	C	1.041252	-0.95614	0.86225
25	C	0.489553	0.218221	0.377393

26	O	0.96124	-3.3895	0.861833
27	C	2.112795	-3.43388	1.732514
28	C	2.432604	-4.8954	1.969976
29	C	3.626871	-5.03069	2.906526
30	C	4.010454	-6.46682	3.158516
31	O	5.013274	-6.54869	4.047767
32	O	3.495771	-7.43472	2.632504
33	C	5.488623	-7.89163	4.369256
34	C	6.597531	-7.74253	5.382503
35	H	2.802422	3.118237	-2.52423
36	H	1.336054	1.297688	-1.91549
37	H	-1.73721	4.109503	-0.8027
38	H	-0.28305	5.949438	-1.37581
39	H	-2.57988	2.900509	-2.81497
40	H	-4.97644	3.091064	-3.04657
41	H	-5.48884	0.436	0.349967
42	H	-3.08829	0.236299	0.536489
43	H	0.818738	7.237272	-2.88247
44	H	1.519937	7.41194	-1.25324
45	H	2.499948	7.765556	-2.69048
46	H	4.129117	4.903264	-2.01475
47	H	3.614967	4.923063	-3.72097
48	H	4.0882	6.431034	-2.91383
49	H	-8.71464	1.286835	-0.93101
50	H	-7.46607	0.050705	-0.69484
51	H	-7.59001	1.422993	0.435512
52	H	-7.1655	2.481572	-3.48485
53	H	-8.4658	2.820853	-2.32577
54	H	-7.00781	3.829906	-2.33013
55	H	-2.01214	-1.07443	-1.52885
56	H	-1.01544	-3.1776	-0.69932
57	H	1.881572	-0.90633	1.544577
58	H	0.905204	1.167856	0.70178
59	H	2.955089	-2.91908	1.250182
60	H	1.87549	-2.92144	2.675189
61	H	1.558793	-5.39522	2.402983
62	H	2.649251	-5.38156	1.012458
63	H	4.509836	-4.52053	2.497921
64	H	3.427927	-4.55763	3.876788
65	H	4.647243	-8.47157	4.763121
66	H	5.837051	-8.36581	3.445562
67	H	6.977933	-8.7341	5.64655
68	H	7.424932	-7.15363	4.975259
69	H	6.233633	-7.2592	6.294182

Table S3. Calculated atomic coordinates of **MG2**.

Atom#	Symbol	X	Y	Z
1	C	0.840098	5.644558	-2.3291
2	C	1.295391	4.310615	-2.48475

3	C	0.4743	3.257146	-2.17621
4	C	-0.85948	3.456163	-1.72856
5	C	-1.30219	4.798641	-1.58543
6	C	-0.48067	5.861062	-1.86028
7	C	-1.71382	2.349408	-1.42423
8	C	-3.13261	2.443547	-1.58851
9	C	-3.71418	3.271854	-2.58535
10	C	-5.07299	3.357096	-2.7478
11	C	-5.94484	2.634752	-1.89375
12	C	-5.37994	1.806017	-0.89116
13	C	-4.01912	1.703878	-0.76077
14	N	-7.27956	2.72938	-2.03497
15	N	1.64575	6.683301	-2.61462
16	C	-1.13236	1.109252	-0.93826
17	C	-1.65632	-0.14324	-1.32842
18	C	-1.0978	-1.3191	-0.87937
19	C	-0.00537	-1.28693	0.004098
20	C	0.52276	-0.05581	0.420019
21	C	-0.03118	1.117821	-0.06203
22	O	0.464468	-2.48855	0.393718
23	C	1.593793	-2.53262	1.294259
24	C	1.911013	-3.99402	1.535021
25	C	3.080466	-4.12922	2.502247
26	C	3.452984	-5.56559	2.769334
27	O	4.459673	-5.64557	3.654157
28	O	2.926458	-6.5351	2.258109
29	C	4.919422	-6.98892	3.996462
30	C	6.028601	-6.837	5.009004
31	H	2.298626	4.133738	-2.86345
32	H	0.83437	2.244321	-2.32911
33	H	-2.29611	4.988231	-1.19166
34	H	-0.82688	6.8792	-1.70295
35	H	-3.06569	3.805441	-3.27368
36	H	-5.495	3.964874	-3.54388
37	H	-6.03891	1.262304	-0.21952
38	H	-3.60954	1.085154	0.031952
39	H	-7.68593	3.322764	-2.74057
40	H	-7.90355	2.208664	-1.43929
41	H	1.322325	7.632401	-2.5163
42	H	2.589574	6.536028	-2.9351
43	H	-2.48611	-0.17906	-2.02812
44	H	-1.48178	-2.28129	-1.20449
45	H	1.349906	-0.00554	1.118192
46	H	0.367832	2.067932	0.281051
47	H	2.446087	-2.01302	0.835391
48	H	1.329701	-2.02464	2.232112
49	H	1.027388	-4.49701	1.9436
50	H	2.153605	-4.47685	0.581922
51	H	3.974402	-3.61934	2.118589

52	H	2.854658	-3.6558	3.46679
53	H	4.071029	-7.55338	4.397673
54	H	5.263782	-7.48052	3.080343
55	H	6.398138	-7.82863	5.287943
56	H	6.862749	-6.26285	4.594499
57	H	5.668586	-6.33675	5.913105

Table S4. Calculated atomic coordinates of **MG3**.

Atom#	Symbol	X	Y	Z
1	C	-3.25423	4.00089	0.047449
2	C	-2.07294	3.648268	-0.66113
3	C	-1.64301	2.347705	-0.67848
4	C	-2.36631	1.308258	-0.03064
5	C	-3.54793	1.680379	0.668335
6	C	-3.97721	2.980185	0.723973
7	C	-1.91589	-0.04816	-0.07295
8	C	-2.83747	-1.13994	-0.01282
9	C	-4.16099	-1.02735	-0.52092
10	C	-5.0415	-2.07639	-0.48535
11	C	-4.65493	-3.31428	0.097785
12	C	-3.33825	-3.44409	0.618887
13	C	-2.46207	-2.39359	0.544038
14	N	-5.50882	-4.33822	0.147365
15	N	-3.67203	5.267348	0.082669
16	C	-0.48907	-0.32315	-0.18286
17	C	-0.01001	-1.3915	-0.97125
18	C	1.340155	-1.64213	-1.08819
19	C	2.266688	-0.84302	-0.3985
20	C	1.816058	0.215406	0.402834
21	C	0.456731	0.468502	0.492364
22	O	3.564661	-1.17208	-0.57057
23	C	4.57216	-0.36045	0.070653
24	C	5.919314	-0.92579	-0.32953
25	C	7.042686	-0.10303	0.288692
26	C	8.412321	-0.62395	-0.06616
27	O	9.372909	0.150481	0.463628
28	O	8.63681	-1.61079	-0.74019
29	C	10.75202	-0.24764	0.195339
30	C	11.64797	0.763432	0.869016
31	C	-3.12807	6.507533	-0.48536
32	C	-4.3301	7.267087	0.138232
33	C	-4.83372	5.91303	0.707134
34	C	-6.89934	-4.49368	-0.29791
35	C	-6.85156	-5.95931	0.212806
36	C	-5.38225	-5.71195	0.650062
37	H	-1.52276	4.414135	-1.19974
38	H	-0.75397	2.095076	-1.24837
39	H	-4.09231	0.923077	1.224457
40	H	-4.8579	3.241196	1.303277

41	H	-4.4628	-0.10398	-1.00602
42	H	-6.03064	-1.97548	-0.92206
43	H	-3.03646	-4.37646	1.08685
44	H	-1.46914	-2.50495	0.96918
45	H	-0.71514	-2.0012	-1.5287
46	H	1.706685	-2.44655	-1.71882
47	H	2.50887	0.832868	0.962283
48	H	0.114029	1.276627	1.132199
49	H	4.465093	0.681327	-0.26224
50	H	4.435047	-0.40049	1.160151
51	H	5.991394	-1.96814	0.000213
52	H	6.007358	-0.91916	-1.42173
53	H	6.989321	0.94579	-0.03157
54	H	6.966821	-0.08695	1.384261
55	H	10.90364	-1.25812	0.589536
56	H	10.90099	-0.27026	-0.88937
57	H	12.69295	0.493672	0.687831
58	H	11.47695	1.767292	0.468739
59	H	11.4788	0.779173	1.949892
60	H	-3.08738	6.50067	-1.58177
61	H	-2.14067	6.76989	-0.08553
62	H	-4.05374	7.998328	0.898168
63	H	-4.99923	7.722913	-0.59191
64	H	-5.79255	5.557044	0.310412
65	H	-4.83877	5.830779	1.801262
66	H	-7.0229	-4.37262	-1.3814
67	H	-7.59885	-3.82975	0.224993
68	H	-7.53466	-6.16957	1.036043
69	H	-6.96633	-6.71052	-0.56889
70	H	-4.62294	-6.29925	0.11875
71	H	-5.1929	-5.76291	1.729571

Table S5. Calculated atomic coordinates of **MG4**.

Atom#	Symbol	X	Y	Z
1	C	-2.72011	3.957993	0.142465
2	C	-1.51222	3.645262	-0.55792
3	C	-1.09129	2.341286	-0.62955
4	C	-1.81431	1.27159	-0.04001
5	C	-3.00269	1.6094	0.658547
6	C	-3.45829	2.899651	0.760696
7	C	-1.35786	-0.07776	-0.13978
8	C	-2.26925	-1.18016	-0.12504
9	C	-1.88182	-2.45179	0.366387
10	C	-2.73802	-3.52513	0.404508
11	C	-4.07499	-3.37692	-0.08413
12	C	-4.47473	-2.11475	-0.62781
13	C	-3.59388	-1.06171	-0.61525
14	N	-4.94692	-4.41451	-0.03457
15	N	-3.15194	5.23632	0.227343

16	C	-2.50563	6.340967	-0.49076
17	C	-4.30618	5.628096	1.043659
18	C	-4.52159	-5.74935	0.397394
19	C	-6.29044	-4.32469	-0.61634
20	C	0.073212	-0.34034	-0.26285
21	C	0.557373	-1.35957	-1.10947
22	C	1.909162	-1.60196	-1.23561
23	C	2.83142	-0.84374	-0.49725
24	C	2.375887	0.166315	0.360644
25	C	1.014756	0.412163	0.459209
26	O	4.132565	-1.16194	-0.68118
27	C	5.132027	-0.40091	0.028808
28	C	6.483957	-0.94409	-0.38624
29	C	7.598879	-0.18241	0.319304
30	C	8.972763	-0.68331	-0.04767
31	O	9.926419	0.032934	0.569603
32	O	9.206161	-1.61113	-0.79807
33	C	11.3083	-0.35537	0.300988
34	C	12.1957	0.579618	1.086446
35	C	-1.69575	5.849814	-1.67609
36	C	-0.73849	4.756992	-1.21261
37	C	-4.7093	3.229782	1.528906
38	C	-4.58863	4.620512	2.142586
39	C	-2.27726	-4.85238	0.950439
40	C	-3.45601	-5.66083	1.47574
41	C	-6.83005	-2.90711	-0.5522
42	C	-5.84582	-1.96385	-1.23225
43	H	-0.19239	2.11967	-1.19906
44	H	-3.54974	0.826283	1.176884
45	H	-0.8825	-2.57592	0.775827
46	H	-3.91026	-0.12091	-1.05838
47	H	-3.29962	7.023654	-0.81865
48	H	-1.86375	6.897074	0.210547
49	H	-5.18606	5.743058	0.391075
50	H	-4.0833	6.614689	1.468675
51	H	-5.40827	-6.27291	0.769651
52	H	-4.14155	-6.31515	-0.46886
53	H	-6.26086	-4.67396	-1.6614
54	H	-6.93689	-5.01117	-0.05902
55	H	-0.14591	-1.9398	-1.69983
56	H	2.278916	-2.36998	-1.90846
57	H	3.065675	0.752459	0.956454
58	H	0.668156	1.183951	1.140653
59	H	5.035472	0.661914	-0.23383
60	H	4.977059	-0.51357	1.110942
61	H	6.541911	-2.00974	-0.13812
62	H	6.59605	-0.85247	-1.4724
63	H	7.558444	0.88938	0.084398
64	H	7.499902	-0.25462	1.410755

65	H	11.43985	-1.39919	0.605264
66	H	11.48517	-0.28145	-0.77726
67	H	13.24255	0.315445	0.907719
68	H	12.04459	1.617754	0.77552
69	H	11.99858	0.498701	2.159664
70	H	-1.15189	6.695413	-2.10828
71	H	-2.3691	5.454134	-2.44706
72	H	-0.15067	4.359048	-2.04606
73	H	-0.02594	5.185265	-0.49207
74	H	-4.88552	2.467415	2.294756
75	H	-5.57481	3.209854	0.850171
76	H	-5.50976	4.907087	2.659249
77	H	-3.7724	4.634846	2.875974
78	H	-1.78311	-5.41949	0.148049
79	H	-1.52653	-4.68928	1.730932
80	H	-3.87938	-5.18089	2.367128
81	H	-3.14383	-6.67176	1.755683
82	H	-6.96995	-2.61513	0.496321
83	H	-7.80823	-2.87514	-1.04215
84	H	-6.17131	-0.92145	-1.1516
85	H	-5.80175	-2.20339	-2.30473

4.5.2 Major MO transitions in excited states

MG1:

1 2.4760 eV 500.74 nm f= 0.99037 Spin multiplicity= 1:
H -> L 99.1%
2 2.8850 eV 429.75 nm f= 0.66465 Spin multiplicity= 1:
H-1 -> L 97.4%
3 3.7790 eV 328.09 nm f= 0.00374 Spin multiplicity= 1:
H-2 -> L 56.0%, H-4 -> L 31.1%, H-3 -> L 8.5%
4 3.8100 eV 325.42 nm f= 0.00081 Spin multiplicity= 1:
H-3 -> L 69.3%, H-4 -> L 27.7%
5 3.8640 eV 320.87 nm f= 0.00676 Spin multiplicity= 1:
H-4 -> L 38.5%, H-2 -> L 36.3%, H-3 -> L 19.0%
6 4.0450 eV 306.51 nm f= 0.00533 Spin multiplicity= 1:
H-5 -> L 96.3%
7 4.3650 eV 284.04 nm f= 0.07382 Spin multiplicity= 1:
H -> L+1 93.1%
8 4.6510 eV 266.58 nm f= 0.15491 Spin multiplicity= 1:
H -> L+2 76.0%, H-1 -> L+1 10.2%
9 4.6740 eV 265.26 nm f= 0.00001 Spin multiplicity= 1:
H-6 -> L 99.9%
10 4.8160 eV 257.44 nm f= 0.06315 Spin multiplicity= 1:
H -> L+3 35.3%, H-1 -> L+1 25.5%, H -> L+2 13.8%, H -> L+4 13.7%
11 4.8560 eV 255.32 nm f= 0.05935 Spin multiplicity= 1:
H -> L+3 42.7%, H-1 -> L+1 29.5%, H -> L+5 10.4%, H-8 -> L 7.0%
12 4.9450 eV 250.73 nm f= 0.04433 Spin multiplicity= 1:
H-8 -> L 39.5%, H-1 -> L+1 24.5%, H -> L+5 13.1%, H -> L+4 9.2%, H-1 -> L+3 6.9%
13 5.0080 eV 247.57 nm f= 0.04488 Spin multiplicity= 1:

H-8 -> L 38.9%, H -> L+5 24.4%, H -> L+4 19.2%

14 5.0890 eV 243.63 nm f= 0.11655 Spin multiplicity= 1:

H -> L+4 46.5%, H -> L+5 36.5%, H -> L+3 6.9%

15 5.2570 eV 235.85 nm f= 0.06879 Spin multiplicity= 1:

H-1 -> L+3 61.0%, H-1 -> L+2 17.6%

16 5.2890 eV 234.42 nm f= 0.02291 Spin multiplicity= 1:

H-1 -> L+2 63.7%, H-1 -> L+3 16.6%

17 5.3250 eV 232.83 nm f= 0.00031 Spin multiplicity= 1:

H-7 -> L 92.7%, H-9 -> L 6.0%

18 5.3800 eV 230.45 nm f= 0.00552 Spin multiplicity= 1:

H-9 -> L 74.9%, H-13 -> L 10.0%, H-7 -> L 6.9%

19 5.4900 eV 225.84 nm f= 0.07440 Spin multiplicity= 1:

H-1 -> L+4 56.4%, H-1 -> L+5 14.9%, H-1 -> L+3 9.0%, H-2 -> L+1 5.8%

20 5.5700 eV 222.59 nm f= 0.01291 Spin multiplicity= 1:

H-1 -> L+5 60.8%, H-1 -> L+4 18.8%, H-1 -> L+2 5.4%

MG2:

1 2.6960 eV 459.88 nm f= 0.81556 Spin multiplicity= 1:

H -> L 98.9%

2 2.9910 eV 414.52 nm f= 0.65016 Spin multiplicity= 1:

H-1 -> L 98.1%

3 3.8350 eV 323.30 nm f= 0.00162 Spin multiplicity= 1:

H-3 -> L 87.9%, H-2 -> L 9.3%

4 3.8480 eV 322.20 nm f= 0.00001 Spin multiplicity= 1:

H-4 -> L 91.7%, H-2 -> L 5.0%

5 4.0540 eV 305.83 nm f= 0.00362 Spin multiplicity= 1:

H-5 -> L 53.9%, H-2 -> L 37.6%

6 4.0970 eV 302.62 nm f= 0.00231 Spin multiplicity= 1:

H-5 -> L 43.7%, H-2 -> L 40.6%, H-3 -> L 6.6%

7 4.5330 eV 273.51 nm f= 0.08063 Spin multiplicity= 1:

H -> L+1 94.0%

8 4.6710 eV 265.43 nm f= 0.00001 Spin multiplicity= 1:

H-6 -> L 99.8%

9 4.8340 eV 256.48 nm f= 0.14794 Spin multiplicity= 1:

H -> L+2 71.6%, H-1 -> L+1 15.8%

10 4.9600 eV 249.97 nm f= 0.01214 Spin multiplicity= 1:

H-1 -> L+1 67.1%, H -> L+2 20.9%

11 5.0240 eV 246.78 nm f= 0.08434 Spin multiplicity= 1:

H -> L+3 71.9%, H -> L+4 6.0%, H-1 -> L+1 6.0%

12 5.1310 eV 241.64 nm f= 0.07237 Spin multiplicity= 1:

H -> L+4 57.5%, H -> L+5 18.4%

13 5.3050 eV 233.71 nm f= 0.13291 Spin multiplicity= 1:

H -> L+5 59.1%, H-1 -> L+2 14.9%, H -> L+4 13.1%

14 5.3270 eV 232.75 nm f= 0.00387 Spin multiplicity= 1:

H-7 -> L 96.8%

15 5.3660 eV 231.06 nm f= 0.02526 Spin multiplicity= 1:

H-1 -> L+3 73.1%, H -> L+4 6.7%, H-1 -> L+2 5.8%

16 5.4360 eV 228.08 nm f= 0.00844 Spin multiplicity= 1:

H-1 -> L+2 56.9%, H-1 -> L+4 8.8%, H -> L+3 7.6%, H-1 -> L+3 5.9%

17 5.4950 eV 225.63 nm f= 0.00457 Spin multiplicity= 1:

H-9 -> L 52.2%, H-1 -> L+5 14.5%, H-13 -> L 13.5%, H-1 -> L+4 6.7%

18 5.5560 eV 223.15 nm f= 0.01984 Spin multiplicity= 1:

H-8 -> L 42.1%, H-10 -> L 34.8%

19 5.6590 eV 219.09 nm f= 0.08441 Spin multiplicity= 1:

H-1 -> L+5 29.2%, H-1 -> L+4 26.3%, H-13 -> L 15.3%, H-1 -> L+3 7.9%

20 5.6940 eV 217.75 nm f= 0.02249 Spin multiplicity= 1:

H-1 -> L+4 38.6%, H-1 -> L+5 30.2%, H-10 -> L 7.9%, H-8 -> L 5.0%

MG3:

1 2.4570 eV 504.62 nm f= 1.08624 Spin multiplicity= 1:

H -> L 99.1%

2 2.9110 eV 425.92 nm f= 0.67788 Spin multiplicity= 1:

H-1 -> L 97.4%

3 3.8290 eV 323.80 nm f= 0.00317 Spin multiplicity= 1:

H-2 -> L 67.1%, H-3 -> L 17.4%, H-4 -> L 9.9%

4 3.8820 eV 319.38 nm f= 0.00186 Spin multiplicity= 1:

H-3 -> L 61.9%, H-4 -> L 31.3%

5 3.9240 eV 315.96 nm f= 0.00504 Spin multiplicity= 1:

H-4 -> L 55.0%, H-2 -> L 21.9%, H-3 -> L 17.1%

6 4.1140 eV 301.37 nm f= 0.00449 Spin multiplicity= 1:

H-5 -> L 96.3%

7 4.2940 eV 288.74 nm f= 0.07217 Spin multiplicity= 1:

H -> L+1 92.6%

8 4.5850 eV 270.41 nm f= 0.16720 Spin multiplicity= 1:

H -> L+2 79.7%, H-1 -> L+1 7.2%

9 4.7420 eV 261.46 nm f= 0.00018 Spin multiplicity= 1:

H-6 -> L 99.8%

10 4.7610 eV 260.42 nm f= 0.09687 Spin multiplicity= 1:

H -> L+3 55.1%, H -> L+4 16.1%, H-1 -> L+1 10.5%, H -> L+2 9.3%

11 4.8120 eV 257.66 nm f= 0.03737 Spin multiplicity= 1:

H-1 -> L+1 42.1%, H -> L+3 22.8%, H -> L+5 16.2%, H -> L+2 6.1%

12 4.9140 eV 252.31 nm f= 0.08678 Spin multiplicity= 1:

H-1 -> L+1 34.0%, H -> L+4 28.2%, H -> L+5 22.9%

13 5.0210 eV 246.93 nm f= 0.10902 Spin multiplicity= 1:

H -> L+4 40.1%, H -> L+5 25.0%, H-8 -> L 17.5%, H -> L+3 7.6%

14 5.0340 eV 246.29 nm f= 0.02754 Spin multiplicity= 1:

H-8 -> L 58.5%, H -> L+5 25.3%, H-1 -> L+3 5.1%

15 5.2340 eV 236.88 nm f= 0.08001 Spin multiplicity= 1:

H-1 -> L+3 42.9%, H-1 -> L+2 33.4%, H-8 -> L 6.0%

16 5.2620 eV 235.62 nm f= 0.02758 Spin multiplicity= 1:

H-1 -> L+2 48.4%, H-1 -> L+3 31.1%, H-1 -> L+4 7.9%

17 5.3890 eV 230.07 nm f= 0.00087 Spin multiplicity= 1:

H-7 -> L 82.2%, H-9 -> L 14.9%

18 5.4270 eV 228.46 nm f= 0.00450 Spin multiplicity= 1:

H-9 -> L 68.0%, H-7 -> L 17.5%

19 5.4710 eV 226.62 nm f= 0.08530 Spin multiplicity= 1:

H-1 -> L+4 50.1%, H-1 -> L+5 20.9%, H-1 -> L+3 9.7%, H-2 -> L+1 5.2%

20 5.5450 eV 223.60 nm f= 0.01952 Spin multiplicity= 1:

H-1 -> L+5 57.0%, H-1 -> L+4 27.6%, H-1 -> L+2 6.2%

MG4:

1 2.3450 eV 528.72 nm f= 1.02989 Spin multiplicity= 1:
H -> L 99.1%
2 2.8750 eV 431.25 nm f= 0.60150 Spin multiplicity= 1:
H-1 -> L 96.9%
3 3.4520 eV 359.17 nm f= 0.00006 Spin multiplicity= 1:
H-2 -> L 67.5%, H-3 -> L 30.2%
4 3.5630 eV 347.98 nm f= 0.00133 Spin multiplicity= 1:
H-4 -> L 86.7%, H-3 -> L 11.0%
5 3.8150 eV 324.99 nm f= 0.02218 Spin multiplicity= 1:
H-3 -> L 53.5%, H-2 -> L 26.9%, H-4 -> L 10.6%
6 4.0270 eV 307.88 nm f= 0.00618 Spin multiplicity= 1:
H-5 -> L 95.8%
7 4.1680 eV 297.47 nm f= 0.07542 Spin multiplicity= 1:
H -> L+1 94.2%
8 4.4430 eV 279.06 nm f= 0.14569 Spin multiplicity= 1:
H -> L+2 87.4%
9 4.6060 eV 269.18 nm f= 0.09454 Spin multiplicity= 1:
H -> L+3 78.2%, H -> L+4 11.0%
10 4.6980 eV 263.91 nm f= 0.01709 Spin multiplicity= 1:
H -> L+5 46.8%, H-1 -> L+1 23.2%, H -> L+4 10.4%, H -> L+2 9.5%
11 4.8240 eV 257.02 nm f= 0.00004 Spin multiplicity= 1:
H-6 -> L 99.9%
12 4.8330 eV 256.54 nm f= 0.05121 Spin multiplicity= 1:
H-1 -> L+1 48.1%, H -> L+4 39.4%
13 4.8500 eV 255.64 nm f= 0.05952 Spin multiplicity= 1:
H -> L+5 36.3%, H -> L+4 31.6%, H-1 -> L+1 18.1%, H -> L+3 5.6%
14 5.0300 eV 246.49 nm f= 0.00003 Spin multiplicity= 1:
H-8 -> L 67.7%, H-1 -> L+3 17.2%, H-10 -> L 6.1%
15 5.1640 eV 240.09 nm f= 0.06989 Spin multiplicity= 1:
H-1 -> L+2 62.7%, H-1 -> L+3 14.1%, H-10 -> L 5.3%
16 5.1760 eV 239.54 nm f= 0.06418 Spin multiplicity= 1:
H-1 -> L+3 50.9%, H-1 -> L+2 20.4%, H-10 -> L 10.6%
17 5.2180 eV 237.61 nm f= 0.00420 Spin multiplicity= 1:
H-9 -> L 65.0%, H-11 -> L 21.3%, H-1 -> L+2 5.1%
18 5.2830 eV 234.69 nm f= 0.00634 Spin multiplicity= 1:
H-10 -> L 67.3%, H-8 -> L 13.5%, H-1 -> L+3 5.8%
19 5.4010 eV 229.56 nm f= 0.01428 Spin multiplicity= 1:
H-1 -> L+4 71.7%, H-8 -> L 5.5%, H-1 -> L+3 5.5%
20 5.4580 eV 227.16 nm f= 0.00737 Spin multiplicity= 1:
H-11 -> L 41.2%, H-7 -> L 19.7%, H-1 -> L+5 18.2%, H-9 -> L 10.7%

4.5.3 Spectra calculation

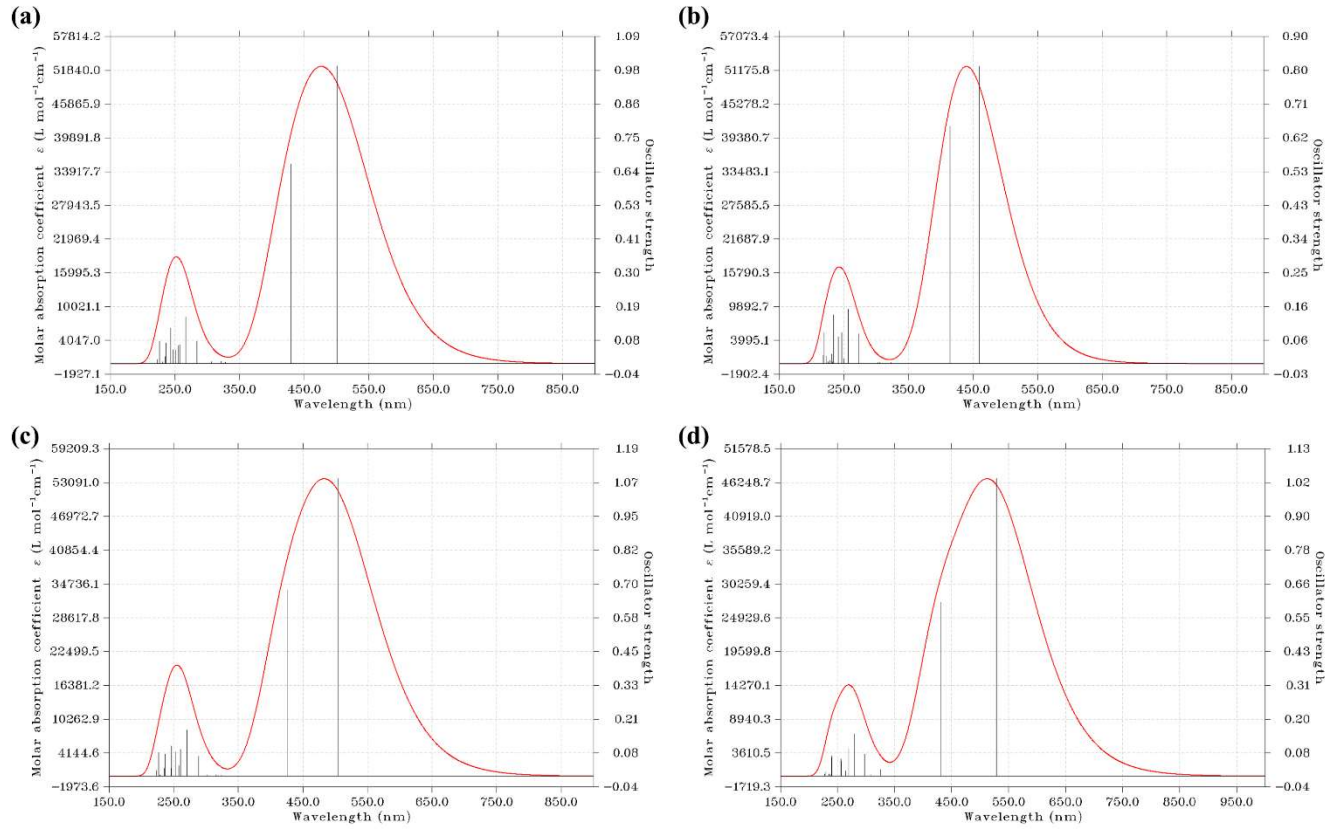

Figure S12. Calculated absorption spectra of (a) **MG1**, (b) **MG2**, (c) **MG3** and (d) **MG4**.

5 Characterization of compounds

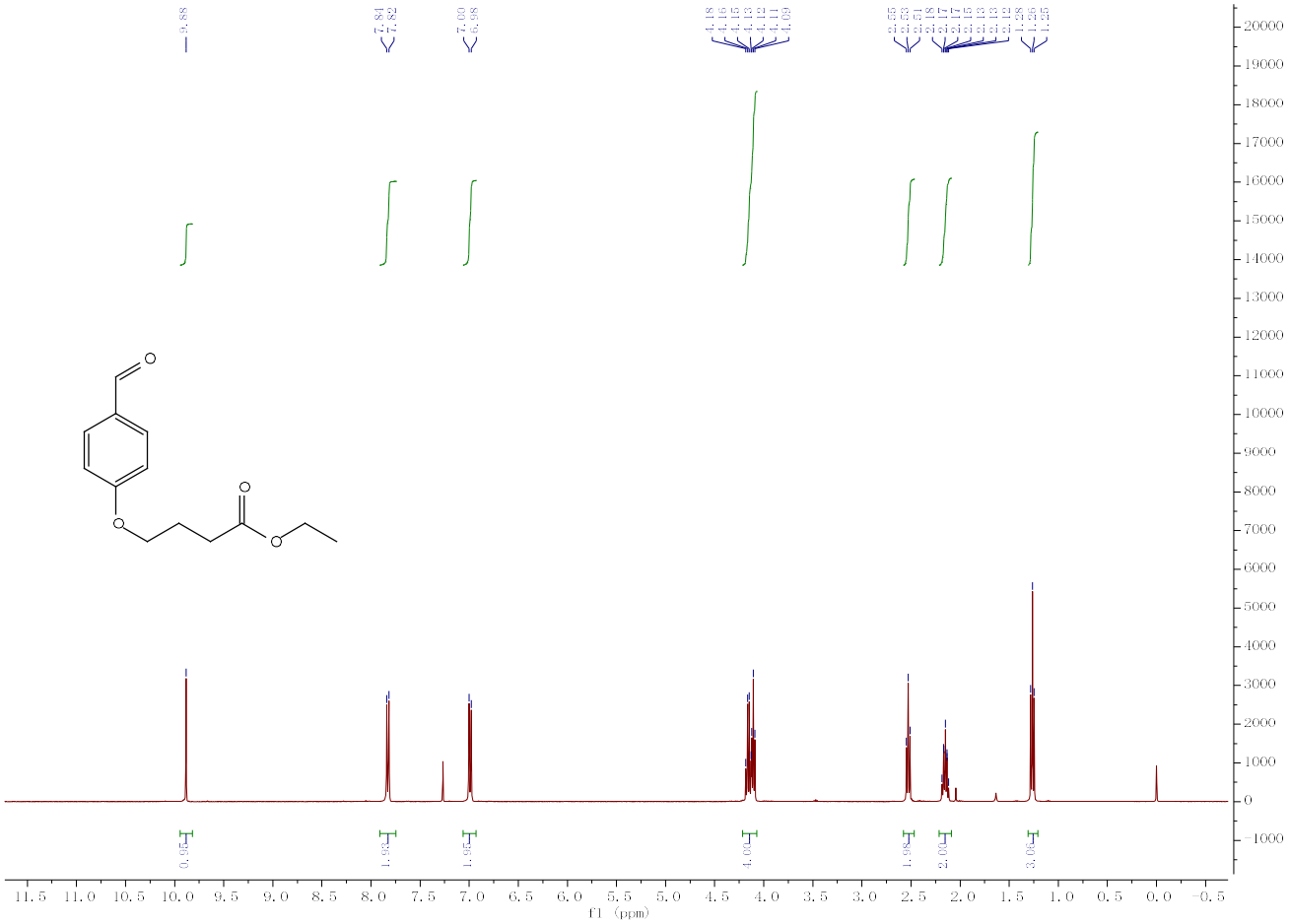

Figure S13. ^{1}H NMR spectrum of **3** in $CDCl_3$.

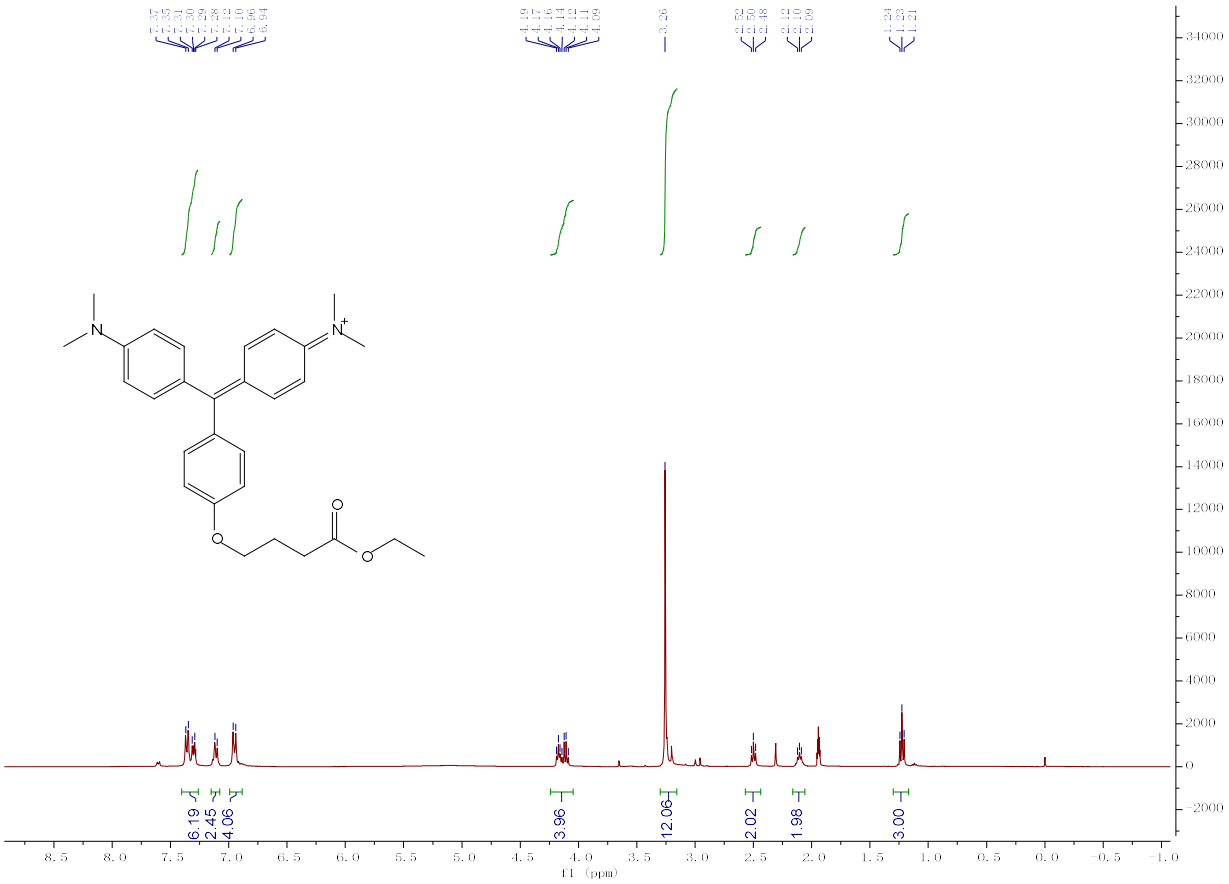

Figure S14. ^{1}H NMR spectrum of **MG1** in $CDCl_3$.

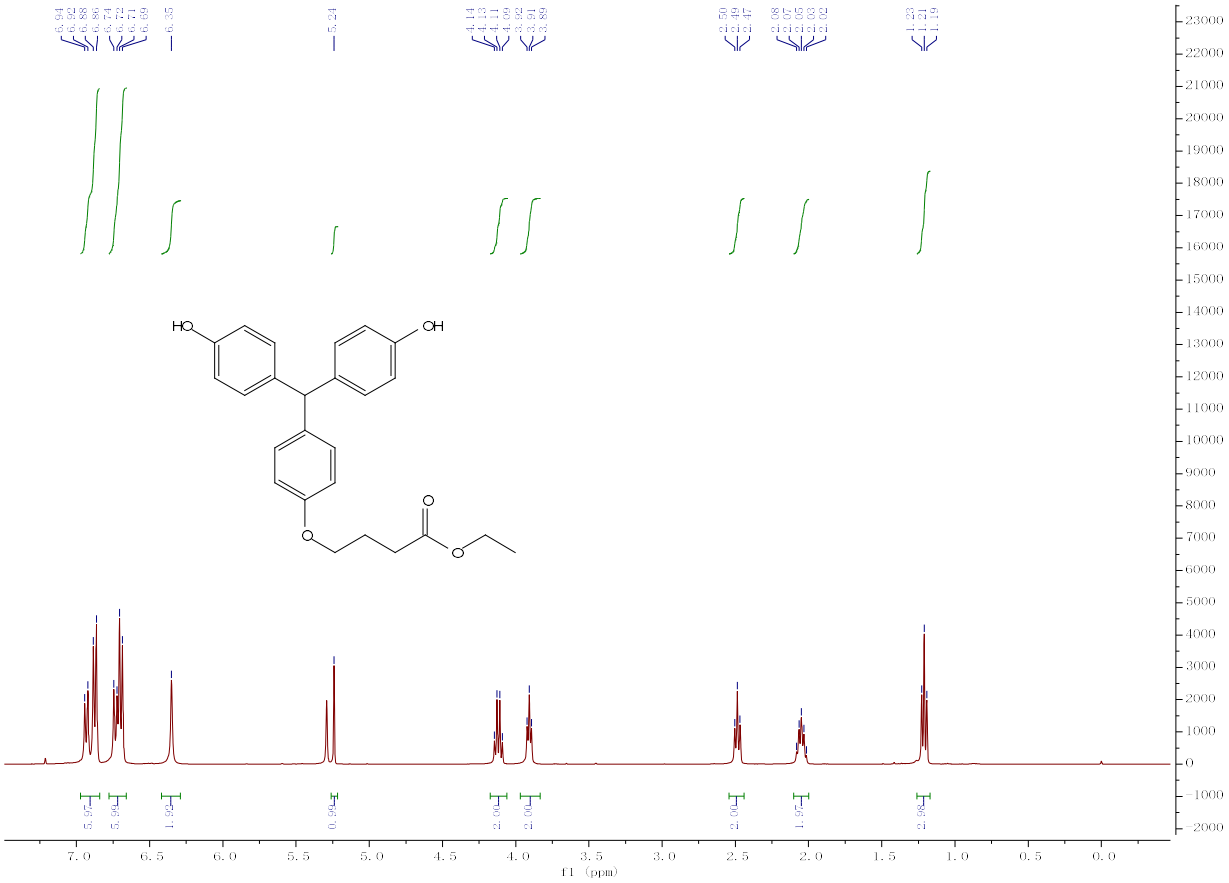

Figure S15. ^{1}H NMR spectrum of **4** in $CDCl_3$.

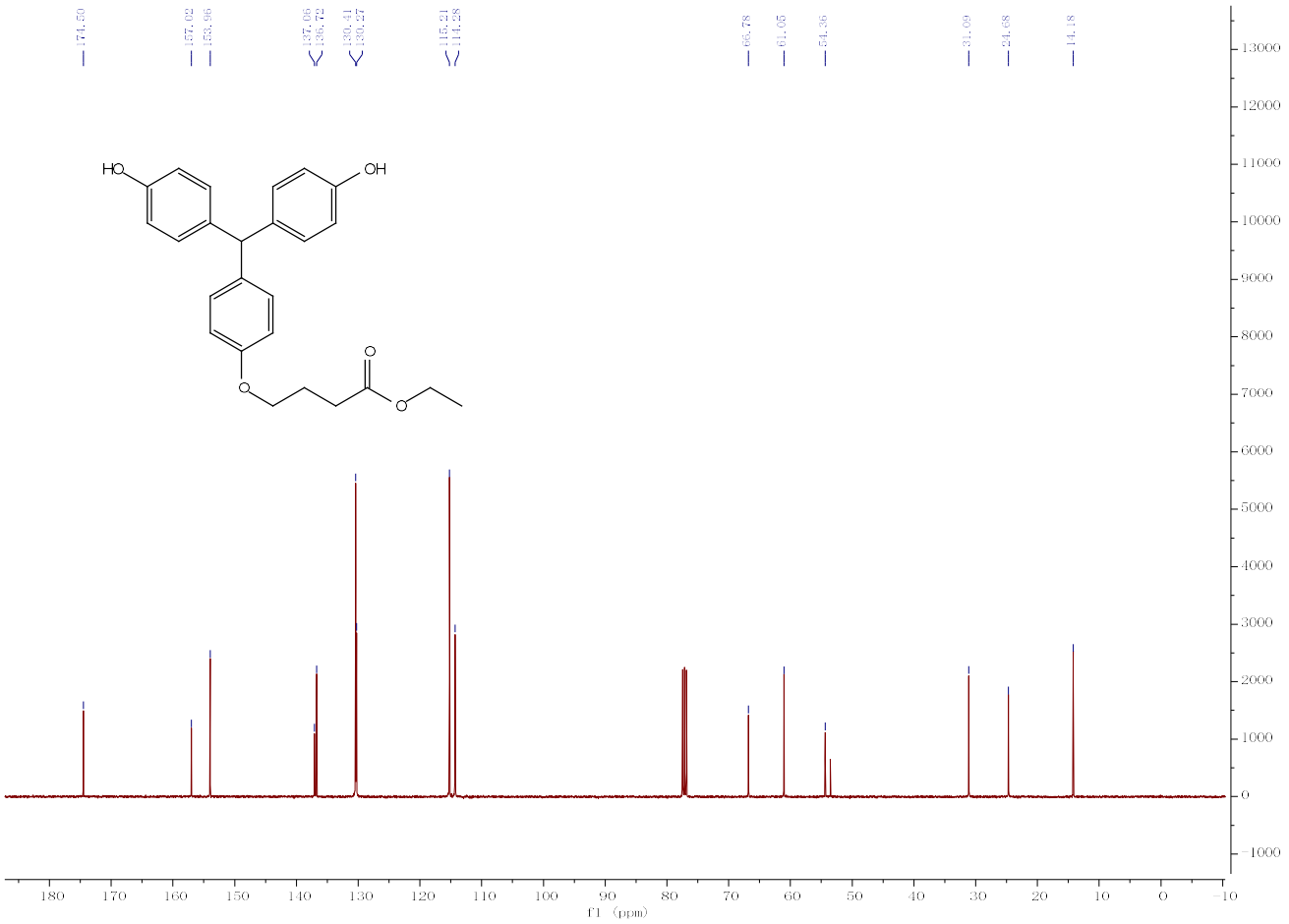

Figure S16. ^{13}C NMR spectrum of **4** in $CDCl_3$.

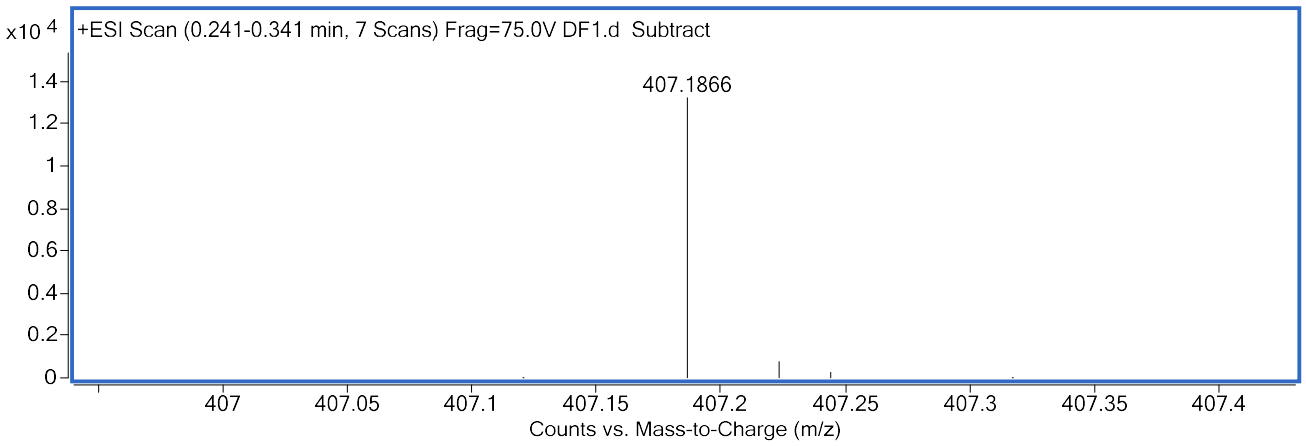

Figure S17. HRMS spectrum of **4** in $CDCl_3$.

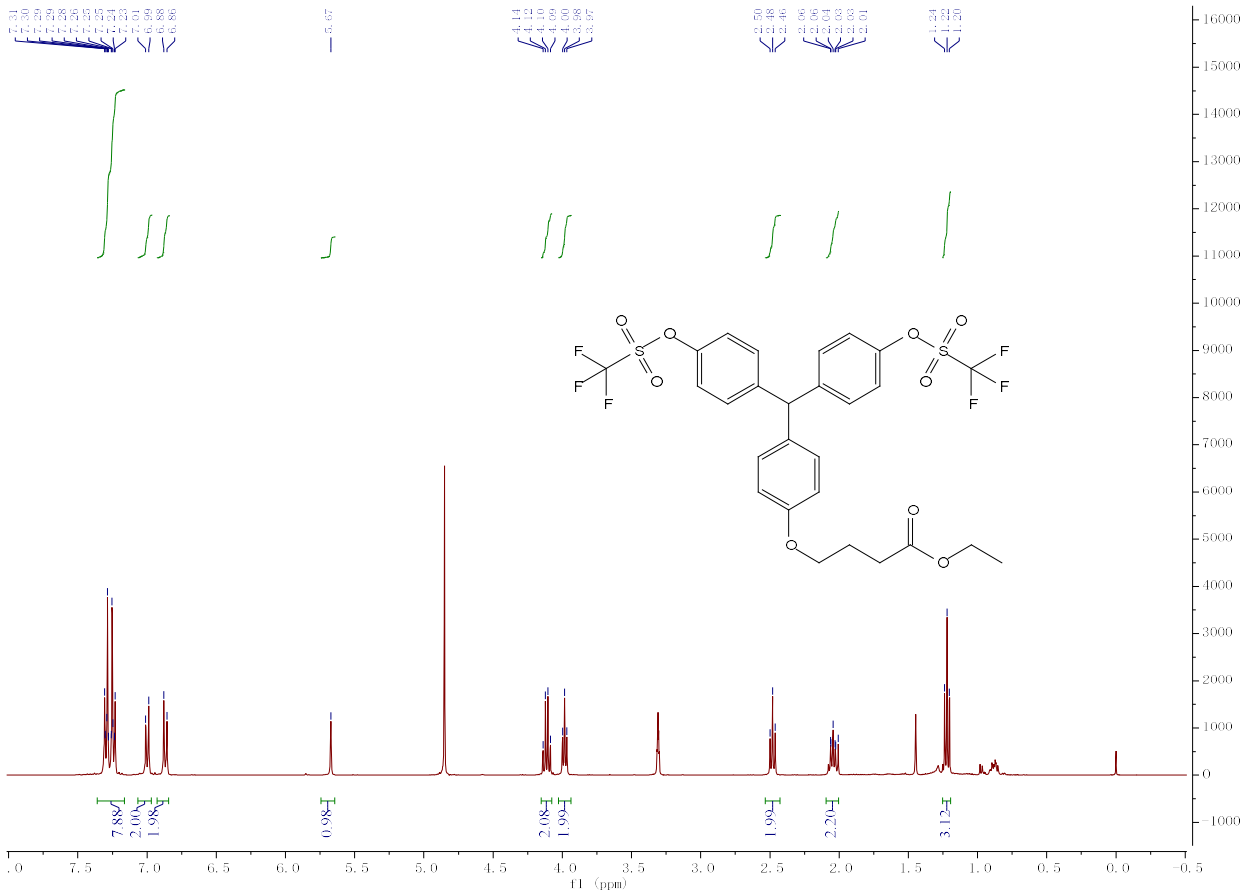

Figure S18. ^{1}H NMR spectrum of **MG1** in CD_3OD.

Figure S19. ^{13}C NMR spectrum of **5** in CD_3OD.

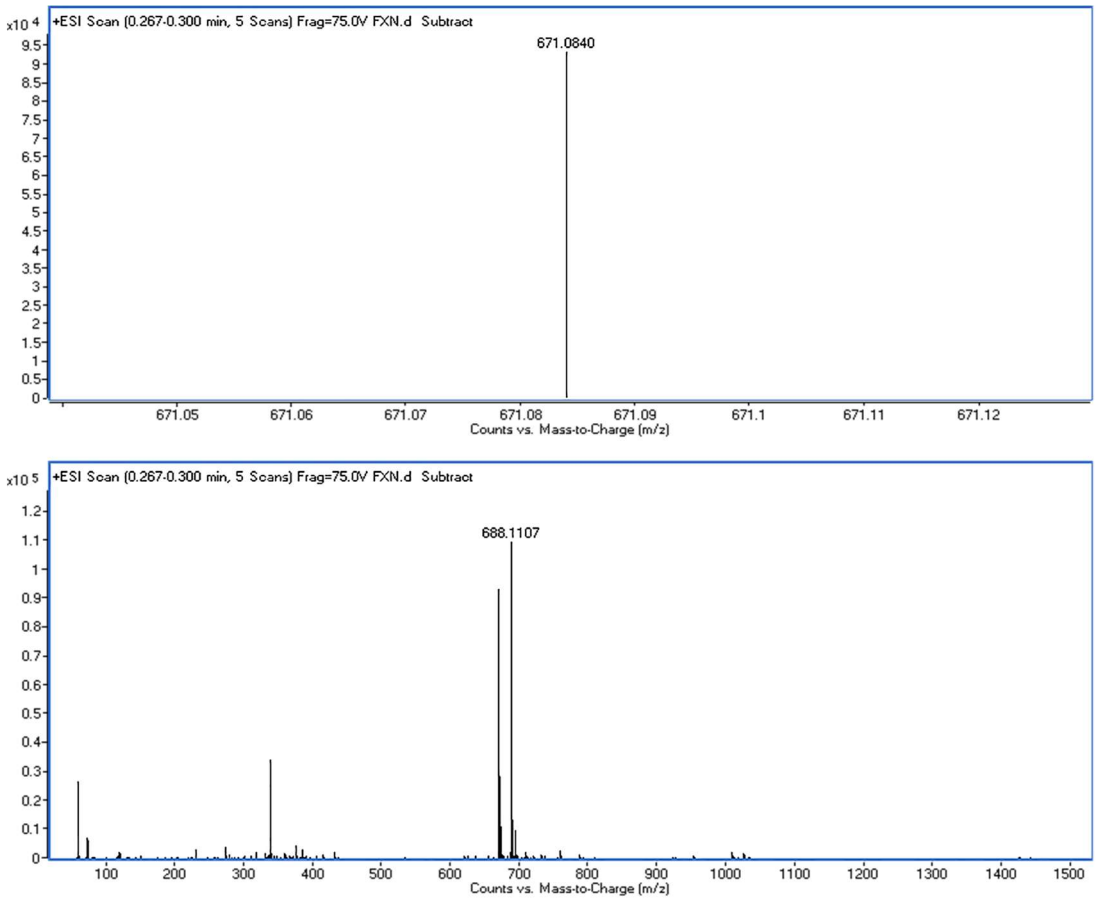

Figure S20 HRMS spectrum of **5**.

Figure S21. ^{1}H NMR spectrum of **6** in $CDCl_3$.

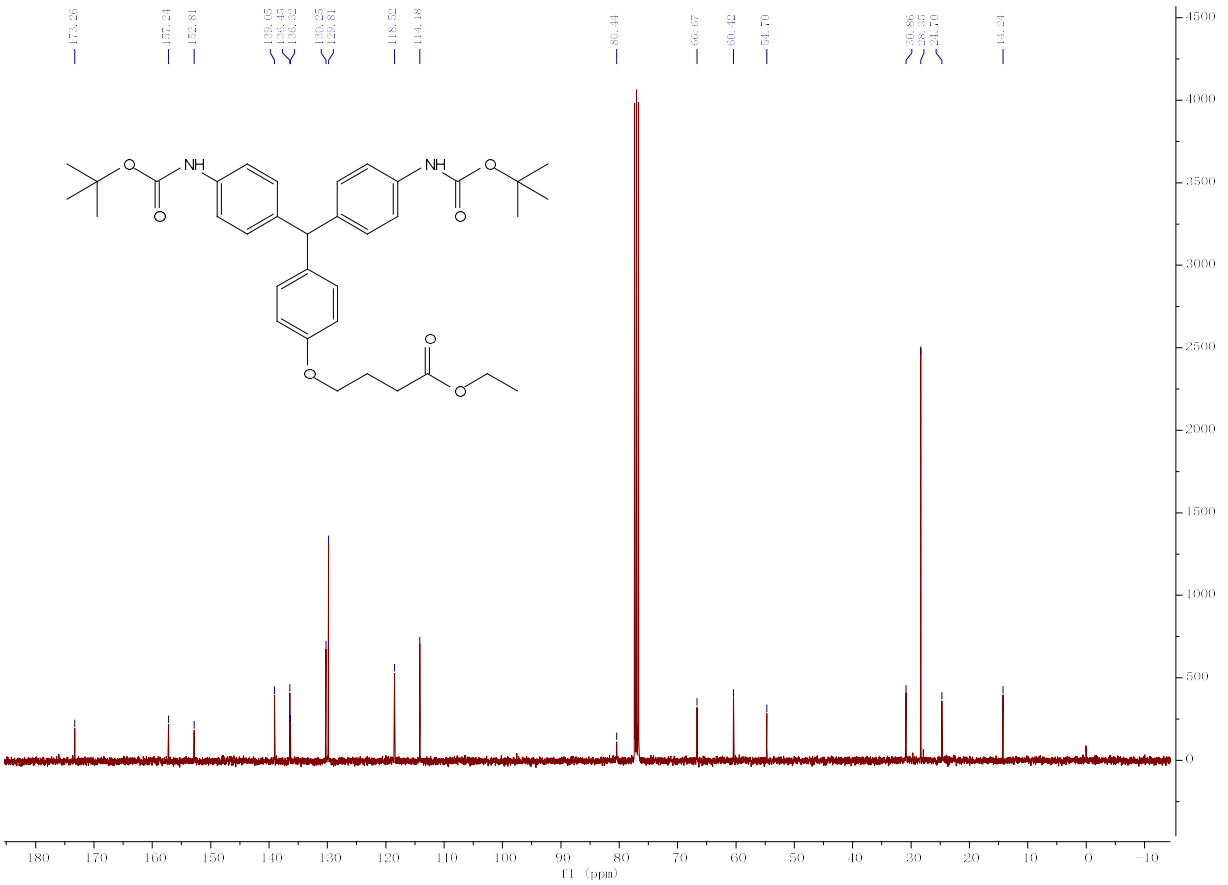

Figure S22. ^{1}H NMR spectrum of **6** in $CDCl_3$.

Figure S23. ^{1}H NMR spectrum of **MG2** in CD_3OD.

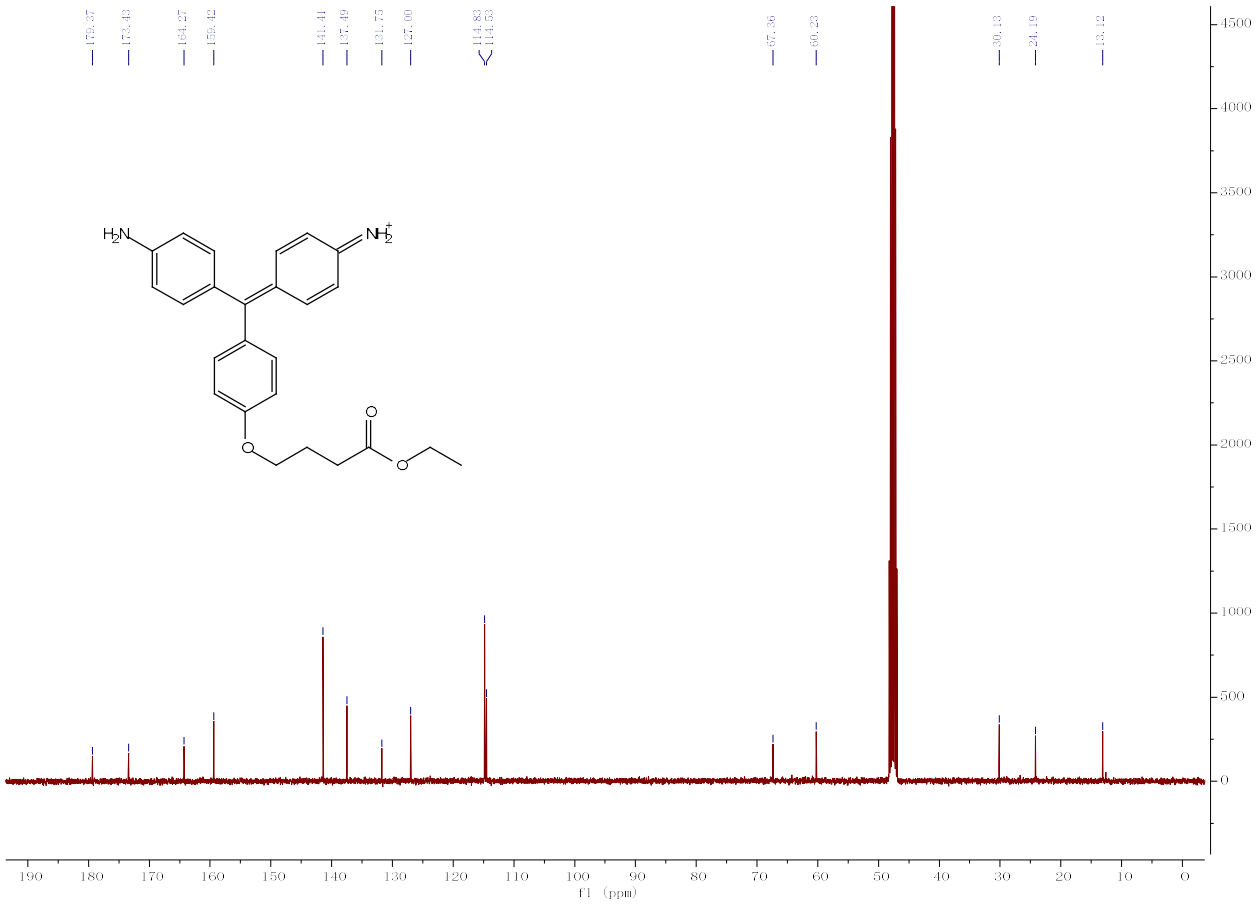

Figure S24. ^{13}C NMR spectrum of **MG2** in CD_3OD.

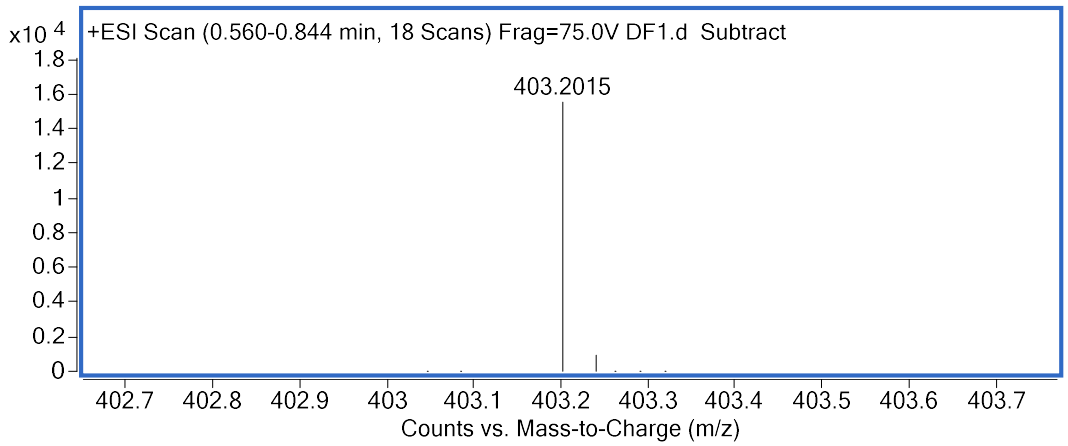

Figure S25. HRMS spectrum of **MG2**.

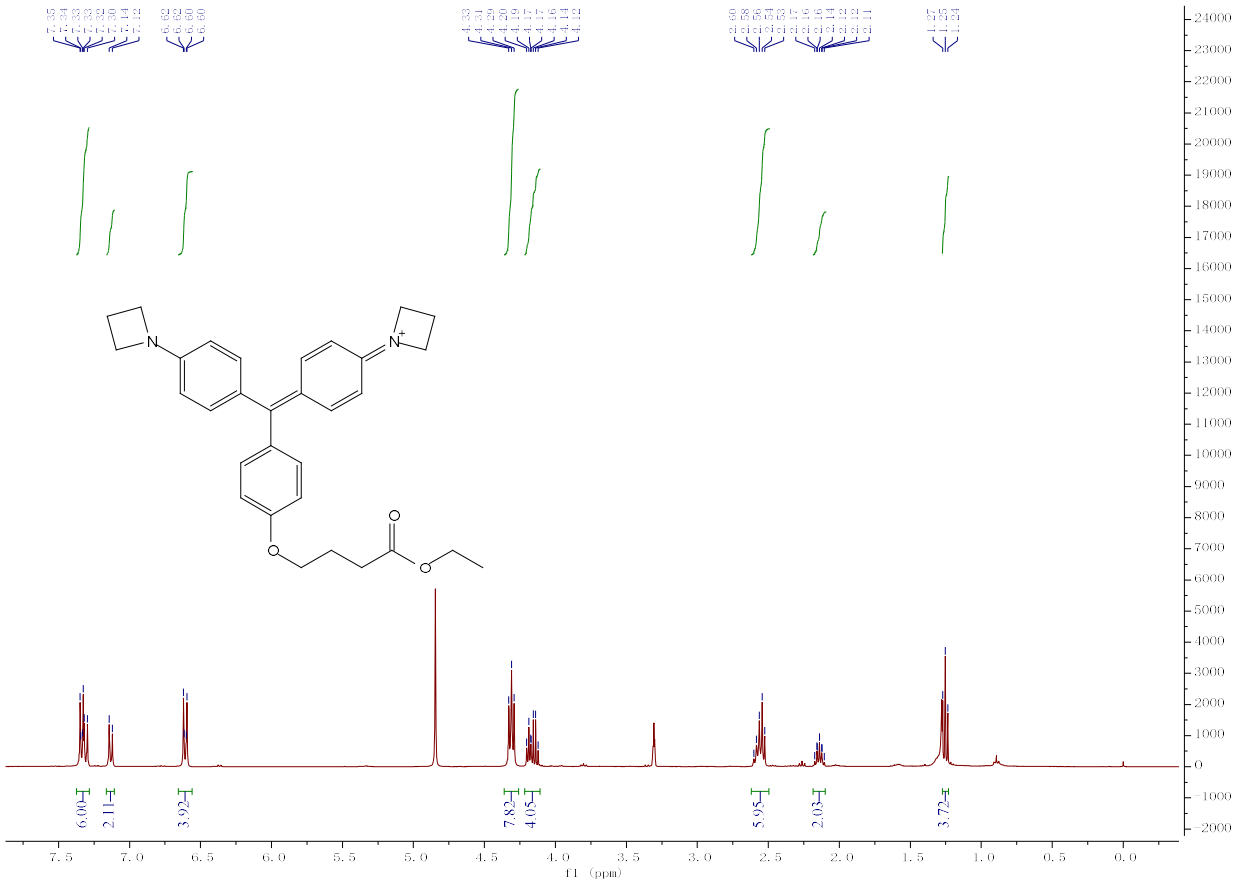

Figure S26. ^{1}H NMR spectrum of **MG3** in CD_3OD.

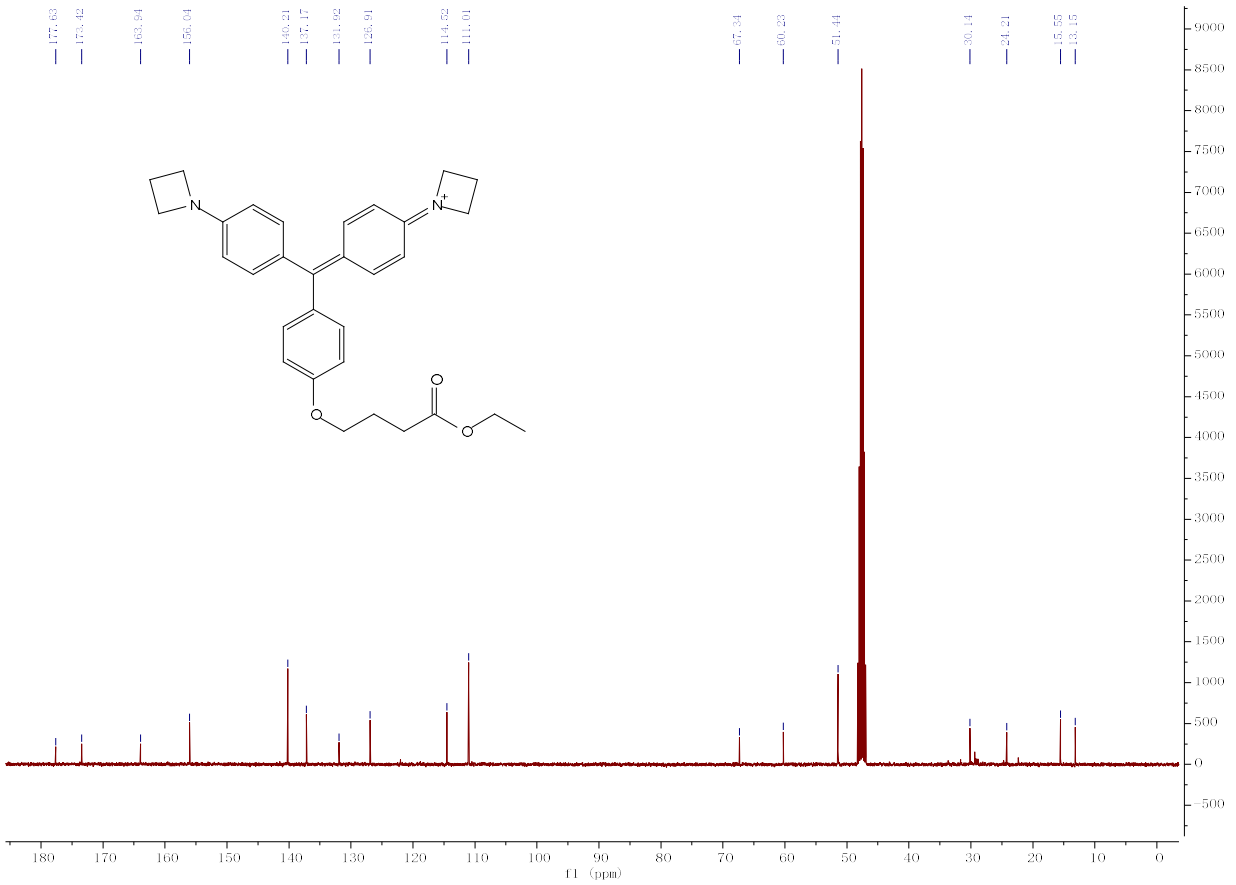

Figure S27. ^{13}C NMR spectrum of **MG3** in CD_3OD.

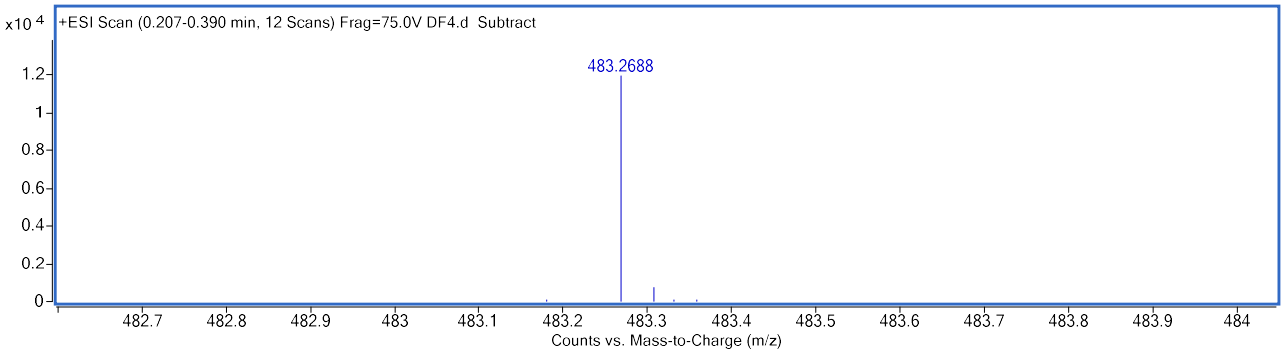

Figure S28. HRMS spectrum of **MG3**.

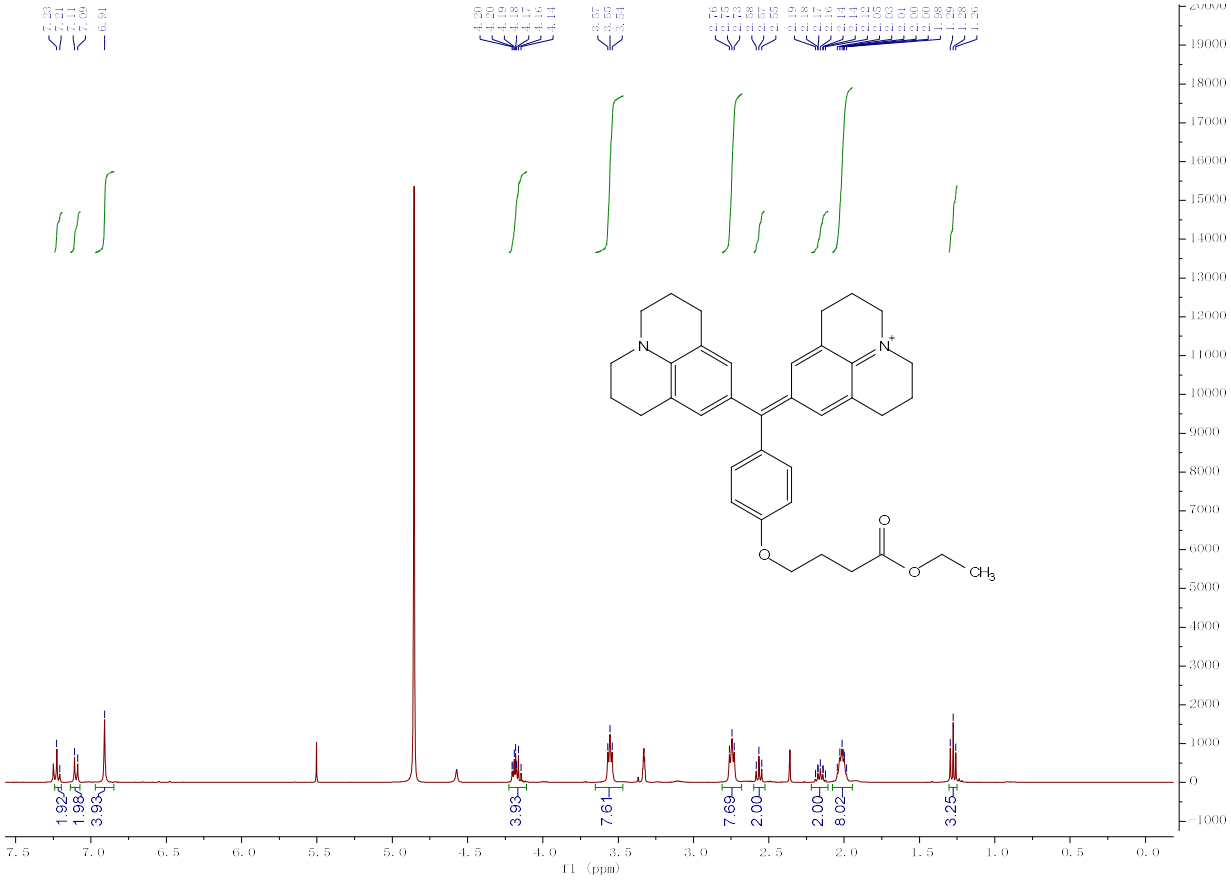

Figure S29. ^{1}H NMR spectrum of **MG4** in CD_3OD.

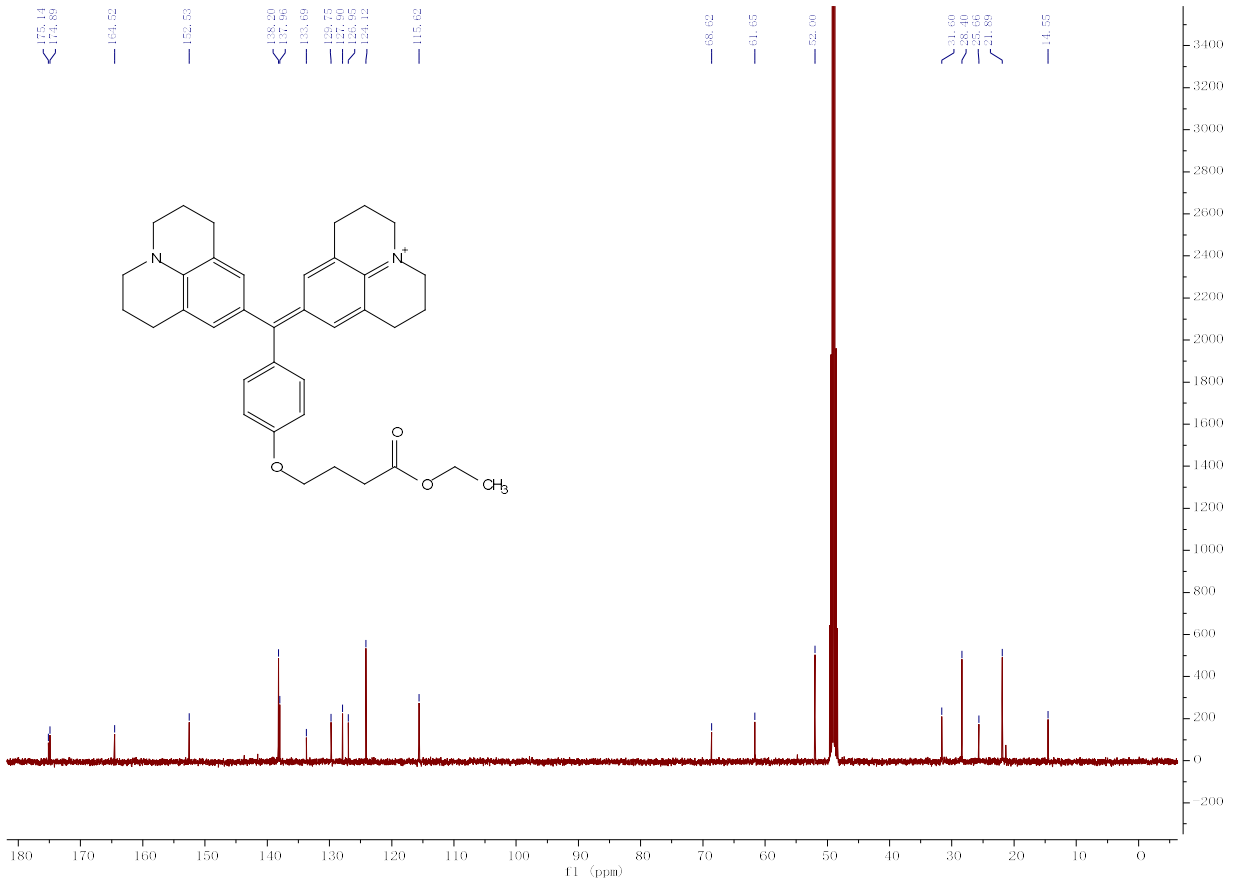

Figure S30. ^{13}C NMR spectrum of **MG4** in CD_3OD.

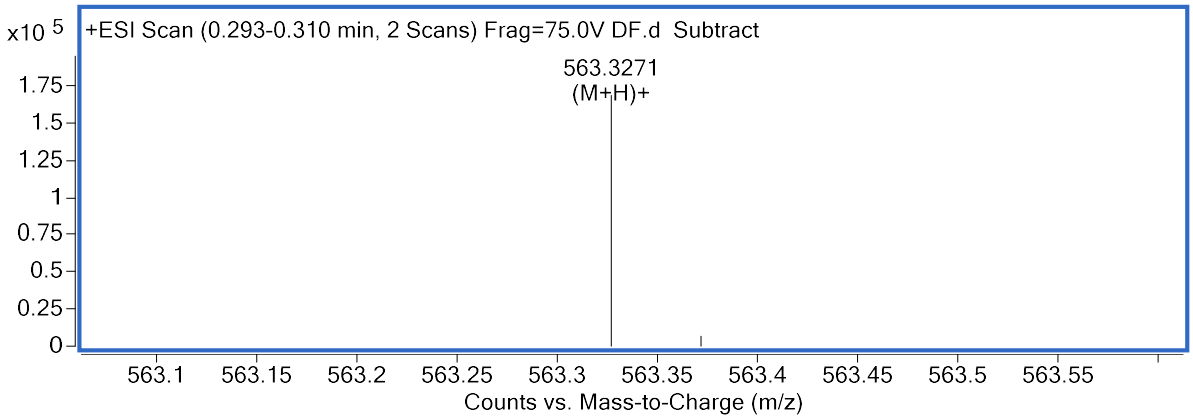

Figure S31. HRMS spectrum of **MG4**.

References

1. G. Wang, T. Chen, T. Peng, S. Zhang, J. Wang, X. Wen, X. Yang and L. Wang, A Strategy To Prepare Peptide Heterodimers in the Solid Phase with an Acid-Labile Linker, *Org. Lett.*, 2019, **21**, 7351-7355.
2. C. Szent-Gyorgyi, B. A. Schmidt, Y. Creeger, G. W. Fisher, K. L. Zakel, S. Adler, J. A. J. Fitzpatrick, C. A. Woolford, Q. Yan, K. V. Vasilev, P. B. Berget, M. P. Bruchez, J. W. Jarvik and A. Waggoner, Fluorogen-activating single-chain antibodies for imaging cell surface proteins, *Nat. Biotechnol.*, 2008, **26**, 235-240.
3. J. B. Grimm, B. P. English, J. J. Chen, J. P. Slaughter, Z. J. Zhang, A. Revyakin, R. Patel, J. J. Macklin, D. Normanno, R. H. Singer, T. Lionnet and L. D. Lavis, A general method to improve fluorophores for live-cell and single-molecule microscopy, *Nat. Meth.*, 2015, **12**, 244-250.
4. F. Neese, The ORCA program system, *Wiley Interdiscip. Rev.: Comput. Mol. Sci.*, 2012, **2**, 73-78.
5. F. Neese, Software update: the ORCA program system, version 4.0, *WIREs Comput. Mol. Sci.*, 2018, **8**, e1327.
6. F. Neese, F. Wennmohs, U. Becker and C. Riplinger, The ORCA quantum chemistry program package, *The Journal of Chemical Physics*, 2020, **152**, 224108.
7. S. Grimme, A. Hansen, S. Ehlert and J.-M. Mewes, r2SCAN-3c: A “Swiss army knife” composite electronic-structure method, *The Journal of Chemical Physics*, 2021, **154**, 064103.
8. T. Lu and F. Chen, Multiwfn: a multifunctional wavefunction analyzer, *J. Comput. Chem.*, 2012, **33**, 580-592.
9. W. Humphrey, A. Dalke and K. Schulten, VMD: visual molecular dynamics, *J Mol Graph*, 1996, **14**, 33-38.
10. A. Waterhouse, M. Bertoni, S. Bienert, G. Studer, G. Tauriello, R. Gumienny, F. T. Heer, T. A. P. de Beer, C. Rempfer and L. Bordoli, SWISS-MODEL: homology modelling of protein structures and complexes, *Nucleic Acids Res.*, 2018, **46**, W296-W303.
11. O. Trott and A. J. Olson, AutoDock Vina: improving the speed and accuracy of docking with a new scoring function, efficient optimization, and multithreading, *J. Comput. Chem.*, 2010, **31**, 455-461.
12. W. L. DeLano, Pymol: An open-source molecular graphics tool, *CCP4 Newsl. Protein Crystallogr*, 2002, **40**, 82-92.